

THE BINDER PHASE IN TITANIUM CARBIDE - NICKEL CERMETS

By

Edward Roy Stover

S. B., Massachusetts Institute of Technology, 1950

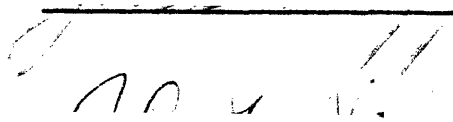
Submitted in Partial Fulfillment of the  
Requirements for the Degree of  
MASTER OF SCIENCE

at the  
Massachusetts Institute of Technology  
1952


Signature of Author  
Department of Metallurgy  
May 16, 1952.

  
\_\_\_\_\_

Signature of Professor  
in Charge of Research.

  
\_\_\_\_\_

Signature of Chairman,  
Departmental Committee  
on Graduate Students.

  
\_\_\_\_\_

## THE BINDER PHASE IN TITANIUM CARBIDE - NICKEL CERMETS

by

EDWARD ROY STOVER

Submitted to the Department of Metallurgy on May 16, 1952 in partial fulfillment of the requirements for the degree of Master of Science.

---

## ABSTRACT

The nickel-rich portion of the system nickel-titanium-carbon above 1200 C was tentatively determined by metallographic examination of samples quenched from different temperatures, supplemented by thermal analysis and by magnetic and X-ray measurements. A quasi-binary eutectic at 1307 C was found between titanium carbide, alpha nickel solid solution containing ten and one-half atomic per cent titanium and one atomic per cent carbon, and liquid containing thirteen atomic per cent titanium and four atomic per cent carbon. A ternary eutectic between alpha, titanium carbide, graphite, and liquid occurs at 1270 C; another ternary eutectic between alpha, titanium carbide, the intermetallic  $\text{TiNi}_3$ , and liquid occurs at 1295 C. Temperatures of the binary eutectics were found to be 1328 C for alpha - graphite - liquid and 1304 C for alpha -  $\text{TiNi}_3$  - liquid. The solubility of titanium carbide together with graphite in alpha decreases from 3.6 atomic per cent titanium and 2.8 atomic per cent carbon at 1270 C to about 3.6 atomic per cent titanium and 1.8 atomic per cent carbon at 1200 C. Two-phase fields form on

solidification between titanium carbide and each of the binary inter-metallics  $\text{TiNi}_3$ ,  $\text{TiNi}$ , and  $\text{Ti}_2\text{Ni}$ . The solubility of nickel in titanium carbide is negligible.

The equilibrium diagram, together with the modifications of the phase boundaries and grain structure produced by non-equilibrium solidification and by oxygen and nitrogen contamination, (revealed by the microstructures), provide a detailed picture of the role of the binder during the sintering of titanium carbide - nickel cermets. Some conclusions of practical importance are: the possibility of sintering in the presence of a partly liquid binder, the possibility of supersaturating the binder in carbon by rapid cooling, and the deleterious effects of oxygen in preventing wetting of the carbide by the binder, forming gas bubbles in the cermet, and displacing carbon as graphite from solution in the carbide.

---

Thesis Supervisor: John Wulff  
Title: Professor of Metallurgy

TABLE OF CONTENTS

	<u>Page</u>
ABSTRACT:	ii
ILLUSTRATIONS:	vi
TABLES:	vi
ACKNOWLEDGMENTS:	vii
I. INTRODUCTION:	1
II. PREVIOUS WORK:	2
A. Phase Relationships in Cemented Titanium Carbide:	2
B. Binary System Nickel - Carbon:	3
C. Binary System Nickel - Titanium:	4
D. Binary System Titanium - Carbon:	5
E. Effects of Oxygen and Nitrogen Contamination:	6
III. EXPERIMENTAL:	8
A. Preliminary Studies:	8
B. Procedure:	11
1. Alloy Preparation:	11
2. Heat Treatment:	12
3. Examination:	14
C. Results:	15
1. Tentative Diagram Nickel-Titanium-Carbon Above 1200 C:	15
2. Phase Shape and Mode of Formation:	21
IV. DISCUSSION AND CONCLUSIONS:	27
A. The Equilibrium Diagram:	27
B. Binder Phase Relationships During Sintering:	29

V. SUMMARY:	32
VI. BIBLIOGRAPHY:	33
VII. SUGGESTIONS FOR FURTHER RESEARCH:	37
VIII. APPENDIX:	39
A. Thermal Analysis:	39
1. Procedure:	39
2. Results:	41
B. Description of Starting Materials:	43
C. Arc Melting Equipment and Procedure:	45
1. Equipment:	45
2. Procedure:	47
D. Data on Important Compositions:	50
E. Appearance of Ingots:	51
F. Chemical Analysis:	56
1. Sampling:	56
2. Carbon:	56
3. Titanium:	56
G. Preparation of Zirconia Boats:	58
H. Heat Treatment Equipment and Procedure:	59
1. Equipment:	59
2. Procedure:	61

# ILLUSTRATIONS

<u>Fig. No.</u>		<u>Page No.</u>
1	Reaction between a 20 wt-TiC/80 wt-Ni compact and an arc-cast TiC block after holding one-half hour at 1340 C and slowly cooling:	9
2	Structures in the 13.7-TiC thermal analysis ingot after melting and solidifying three times in zirconia under impure argon:	10
3	Nickel-Titanium-Carbon diagram projected onto a basal plane at 1200 C (atomic pct scale):	16
4	Vertical sections across the $\alpha$ + TiC field showing data obtained:	17
5	Vertical section between pure nickel and commercial TiC (49.5 atomic pct carbon):	18
6	Important binary microstructures (reduced one-half):	22
7	Important as-cast microstructures (reduced one-half):	23
8	Important annealed microstructures (reduced one-half):	24
9	Vertical sections through ternary Ni-Ti-C diagram at and near the TiC - Ni plane:	28
10	Arc Melting Chamber:	46
11	Typical ingot surfaces:	52
12	Surface of Fig 11 J(21.2 atomic pct C, 20.9 atomic pct Ti, bal Ni) at 450 X:	53
13	Particle in the nickel - titanium binary sample melted with a graphite electrode:	54
14	Arrangement of apparatus for heat-treating samples:	60

# TABLES

I. Features of the System Ni-Ti-C:	19
II. Data from Thermal Analysis:	42

## ACKNOWLEDGMENTS

The author wishes to express his sincere appreciation to Professor John Wulff and Dr. James E. Cline for their continued assistance, inspiring advice, and very helpful criticism in patiently guiding this research. Among the many others who have unselfishly contributed to the completion of this work, special thanks are due to Malcolm Basche, Romeo G. Bourdeau, Richard H. Foss, Robert L. Jones, James H. Johnston, William A. Moffatt, Robert M. Rodgers, and Phyllis M. Stratton. Financial support was provided by the Wright Air Development Center.

## I. INTRODUCTION

In the search for new materials capable of resisting the drastic service conditions of jet engine turbine blades, extensive studies have been made of the "cermets", also called "ceramals", "metamics", or "metal ceramics". These are bodies composed of fine grains of an oxide or an interstitial compound "cemented" together by a metal or alloy of iron group elements. Among such alloy mixtures, titanium carbide - nickel compositions have demonstrated many advantages, such as good resistance to thermal shock and oxidation, superior strength - weight ratios, and the use of materials readily obtained by the United States.

Titanium carbide - nickel bodies are prepared, like other cemented carbides, by sintering or infiltrating pressed compacts at temperatures above the solidus of the alloy. To aid in understanding the variables involved in sintering or infiltrating and their effects on the final properties, a limited study of the system nickel-titanium-carbon has been made. The equilibrium relationships in the vicinity of the solidus, together with the effects of cooling rate and contamination in modifying both the equilibrium and the grain structure, provide a detailed picture of the roll of the binder phase in cermets of this type.



## II. PREVIOUS WORK

### A. Phase Relationships in Cemented Titanium Carbide.

Although the manufacture and properties of titanium carbide cemented by nickel, cobalt, and various alloys have been described in detail, no previous investigation of the phase system has been made. Free graphite is frequently encountered in commercial alloys, but gradient studies<sup>1</sup> have shown that no intermediate phase exists between nickel and titanium carbide, which is usually termed "TiC".

Eutectic between carbide and metal: Trent, Carter and Bateman,<sup>2</sup> in studying TiC - nickel cermets with small additions of  $\text{Cr}_3\text{O}_2$ , noted that liquid started to form between 1200 and 1300 C. Bourdeau<sup>3</sup> reported that a plate-like eutectic structure containing  $9 \pm 0.5$  per cent TiC by weight resulted from slowly cooling ingots made from 10 per cent TiC - 90 per cent nickel powder mixtures, and that pieces cut from such a structure melted at  $1300 \pm 10$  C.

Solubility of carbide in metal: Polikarpova<sup>4</sup> reported that cobalt dissolves 7 to 10 per cent TiC by weight between 1150 and 1250 C, but Zarubin and Molkov<sup>5</sup> could find no solubility in nickel by metallographic examination. Nickel has been reported to dissolve up to 20 per cent TaC, 12 per cent  $\text{Mo}_2\text{C}$ , 8 per cent  $\text{Cr}_3\text{O}_2$ , and 15-30 per cent WC by weight.<sup>5-8</sup>

Solubility of metal in carbide: Work in Germany<sup>9</sup> indicated that cobalt dissolves in TiC, and Kieffer has stated<sup>10</sup> that solid solutions of group IV carbides with group VI carbides (WC dissolved in TiC, for example) can dissolve 3 to 5 per cent nickel or cobalt at

room temperature. However, Metcalfe<sup>11</sup> found "no evidence from either X-ray diffraction data or spectroscopic analysis of carbides extracted from sintered products to suggest that WC, TiC, or their solid solution dissolves cobalt."

#### B. Binary System Nickel - Carbon.

The diagram compiled by Kihlgren and Eash<sup>12</sup> is probably correct with respect to the eutectic composition (2.2 weight per cent carbon) and the solubility of carbon in nickel (0.65 weight per cent at 1318 C.) However, the eutectic temperature (1318 C) is based on early thermal analysis measurements which were subject to considerable error. Three groups of investigators<sup>13-15</sup> cooled 20 to 25 gram hypoeutectic melts at 1 to 2 degrees C per second, and the eutectic arrests obtained varied between 1298 and 1325 C, due to supercooling and impurities. Kase's highest value of 1318 C<sup>15</sup> was taken by the reviewers as the best eutectic temperature.

Better results have been recently obtained by Morrogh and Williams<sup>16</sup> who solidified hypereutectic alloys made by melting pure nickel shot in graphite at cooling rates of about 16 degrees C per minute. Arrests at 1323 to 1326 C occurred for alloys which solidified with the "undercooled graphite" eutectic or, when treated with calcium silicide, with nodular graphite. Both types of structures should form below the true equilibrium eutectic. Coarse graphite structures, forming between 1310 and 1330 C, occurred after varying additions of sulfur, and increasing sulfur should lower the solidus. The authors show a good arrest at 1328 C for an alloy containing 0.3 per cent

sulfur and forming coarse graphite on solidification; this value, rather than 1318 C, is the best present value for the eutectic. Most errors in thermal analysis tend to yield low temperatures, and the early workers did not realize the effects of nucleation on the graphite solidification temperature.

Although an inflection in the liquidus at 2100 C occurs at 25 atomic per cent carbon,<sup>14</sup> a solid carbide of nickel can be obtained only by quenching superheated melts or by chemical reaction around 170 to 250 C.<sup>17-18</sup> This hexagonal-close-packed, paramagnetic structure dissolves carbon interstitially up to a maximum corresponding to the formula  $\text{Ni}_3\text{C}$ . Upon heating in vacuum, it decomposes at 210 C into a metallic interstitial phase of nickel supersaturated with carbon. This transition " $\text{Ni}_4\text{C}$ " has a higher lattice parameter and a lower Curie point than the solid solution in equilibrium with graphite.<sup>18</sup>

#### C. Binary System Nickel - Titanium.

Three stable intermetallics occur in this system:

- (a)  $\text{Ti}_2\text{Ni}$ , decomposing at 1015 C,<sup>19</sup> has the complex cubic structure isomorphous with the eta phase in the wolfram-carbon-cobalt and similar systems. It has been reported to dissolve oxygen to the composition  $\text{Ti}_4\text{Ni}_2\text{O}$ .<sup>20</sup>
- (b)  $\text{TiNi}$ , melting at 1240 C,<sup>19</sup> has a brittle, cesium chloride structure.<sup>21</sup>
- (c)  $\text{TiNi}_3$ , melting at 1378 C, is a fairly tough, closely-packed hexagonal Laves phase, having layers in the order

ABACABAC.<sup>22</sup>

Only the region between titanium and  $\text{TiNi}_3$  has been accurately determined using pure materials.<sup>19</sup> The nickel -  $\text{TiNi}_3$  region, of greatest interest here, is shown by Skinner<sup>23</sup> as determined by Vogel and Wallbaum.<sup>24</sup> Their diagram is undoubtedly inaccurate, as it is based on cooling curves, obtained at 1 to  $1\frac{1}{2}$  degrees C per second, on 20-gram melts made from "nickel wire" and 95 per cent pure titanium in pythagoras crucibles under argon. Their results indicate a eutectic at 1287 C and 16.2 weight per cent titanium, and a solubility in nickel of 10.8 weight per cent titanium at 1287 C, 7 per cent at 1200 C, and 3 per cent at 850 C.

#### D. Binary System Titanium - Carbon.

The solubilities of carbon in alpha and beta titanium<sup>25</sup> and of titanium in "TiC" (about 22 to 26 atomic per cent between 1800 C and 900 C)<sup>25-27</sup> are the only portions of this system which have been accurately determined to date. Approximate measurements indicate that the solidus varies from about 1800 C (peritectic with beta titanium)<sup>28</sup> to a maximum near 3250 C.<sup>29</sup> Hot pressing data indicates that the TiC-graphite eutectic lies between 1900 and 3000 C, probably about 2500 C.<sup>30</sup>

The only carbide, "TiC", is a face-centered-cubic-interstitial structure (type B1), which has a very high modulus and good conductivity. The interstitial lattice is apparently more completely filled at higher temperatures and lower pressures,<sup>31</sup> but the stoichiometric composition in carbon (20.05 weight per cent) is difficult to achieve. The carbon solubility limit when in contact with amorphous carbon may be as high as 19.5 weight per cent, but the equilibrium with graphite is

apparently lower.<sup>32</sup>

#### E. Effects of Oxygen and Nitrogen Contamination.

Since oxygen and nitrogen are usually present in commercial TiC, their effects on the binary carbide are very important. Both elements readily displace carbon in the interstitial lattice, lowering the parameter, the solidus, and the modulus.<sup>35-36</sup> The solubilities increase with decreasing temperature and increasing pressure of the gas in equilibrium with the solid.<sup>31-32</sup> The carbide is oxidized in air at lower temperatures (1200 C), but nitriding takes place more readily at the higher temperatures (1800 C.)<sup>31</sup> Diffusion of nitrogen through the lattice is apparently quite slow.<sup>31</sup> Although TiC, TiN, and TiO may form a continuous series of solutions at the higher temperatures, a gap in the TiC - TiO system appears to exist at lower temperatures in the vicinity of 8 weight per cent carbon.<sup>34</sup> As the ionic character of the bonding changes, the color of the phase may also change; TiC-rich solutions are uniformly light gray, but TiO may vary between yellow and black,<sup>37</sup> and a pink compound in titanium steels has been identified with TiN.<sup>38</sup>

Dissolved oxygen is particularly deleterious for cemented carbides; it inhibits wetting by a binder such as cobalt, forcing the use of higher sintering temperatures. At temperatures sufficiently above the solidus, solution and "recrystallization" of carbide through the binder results in a copious evolution of CO, which leads to porosity in the center of the body.<sup>39</sup>

Hydrogen also dissolves interstitially in TiC,<sup>40</sup> and this gas may decarburize the phase by a slight amount through the formation of

hydrocarbons, under the proper conditions of temperature and pressure.<sup>32</sup>

### III. EXPERIMENTAL

#### A. Preliminary Studies.

Due to the outstanding stability of TiC among the binary systems, a quasi-binary section possessing an invariant eutectic line between this phase and pure nickel was anticipated. Consequently, studies were first made with TiC - nickel powder mixtures.

Figure 1 shows the result of melting a pressed compact containing 20 per cent of an 18.7 weight per cent carbon TiC on the original surface of a TiC-graphite block (arc-cast at du Pont) in argon containing 0.1 per cent nitrogen. The eutectic structures, the preferential solution of graphite, the "recrystallization" of carbide through the liquid, and the lack of wetting of a contaminated surface layer are evident. When the combination was tipped on its side and reheated, movement of the edge of the casting was observed at  $1290 \pm 15$  C.

Thermal analysis of nickel - TiC powder mixtures containing 10 and 13.7 per cent TiC in zirconia under argon was conducted at cooling rates of 14 to 26 degrees C per minute. Solidification occurred between measured temperatures of 1240 and 1300 C. The initial melting of a powder mixture took place 40 to 50 degrees higher, but good agreement was found between cooling curves and heating curves of previously melted ingots. See Appendix A for details.

Since the thermal analysis ingots were severely contaminated with gases absorbed from the refractory and from the atmosphere, additional phases besides TiC, graphite, and alpha nickel were formed. Figure 2-A

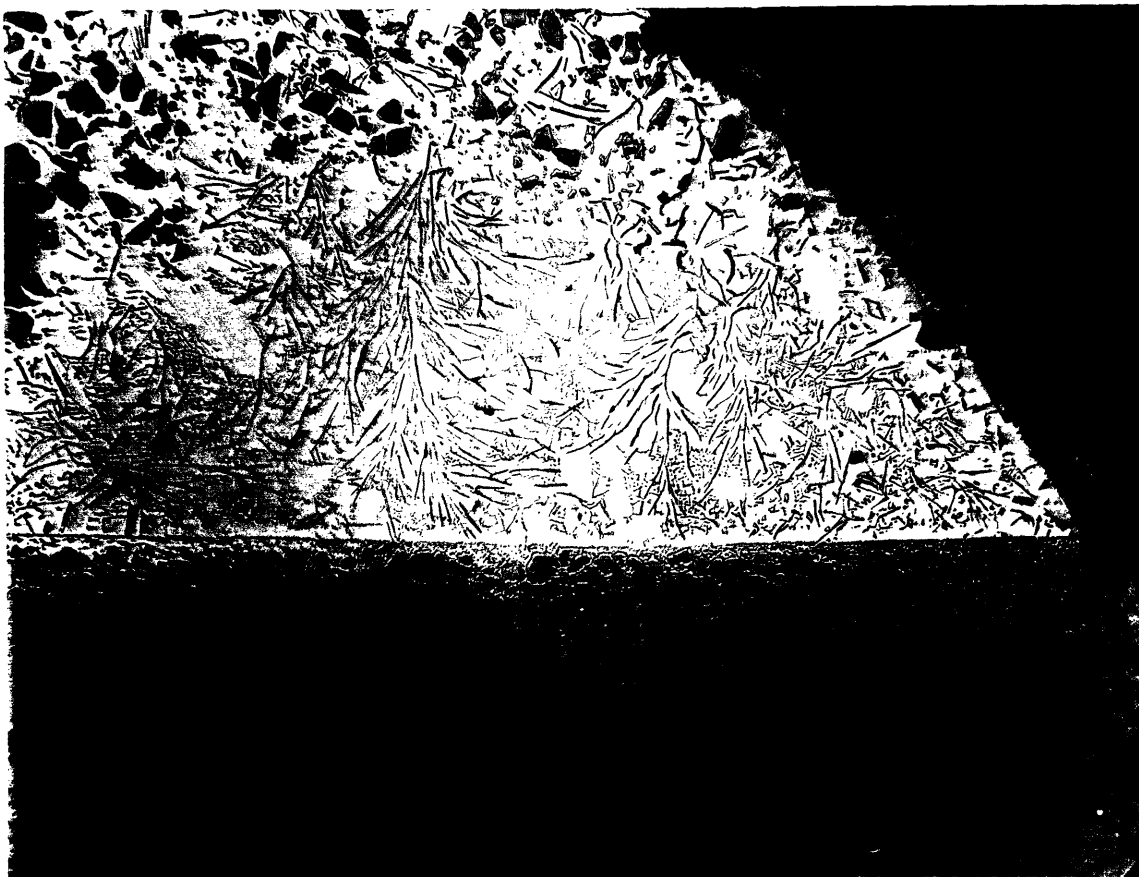


Fig 1 - Reaction between a 20 weight pct TiC, 80 weight pct Ni compact and an arc cast TiC block after holding one-half hour at 1340 C and slowly cooling. Unetched. 50 X.

Notice (from the bottom):

- (a) Original block structure: carbide dendrites in a carbide - graphite eutectic;
- (b) Diffusion region of graphite solution and growth of carbide grains through the liquid;
- (c) Undissolved interface and angle of contact between the liquid and the block surface;
- (d) Structure of the solidified liquid: flake graphite, carbide eutectic, and alpha (nickel) dendrites;
- (e) Undissolved carbide grains floated to the top of the liquid.





A - Partially dissolved carbide grain. 1000 X.



B - Eutectic structures at bottom of ingot. 500 X.

Fig 2 - Structures in the 13.7 weight pct TiC thermal analysis ingot after melting and solidifying three times in zirconia under impure argon. Carapella's reagent.

shows dark gray phases, probably resulting from oxygen, associated with lighter TiC and black graphite. (Note also the precipitate from the inter-carbide alpha.) Figure 2-B shows not only the TiC eutectic associated with graphite in the bottom of the ingot, but a finer, softer, pinkish eutectic of another phase, which shows much less tendency to develop the cubic symmetry of TiC on solidification. (Margolin and Nielsen<sup>41</sup> show identical eutectic structures, similarly associated, in a contaminated 10 per cent titanium - 90 per cent nickel arc cast ingot.) In addition, the 19.6 per cent carbon TiC used in the mixtures contained some of the rose-colored grains frequently encountered in commercial carbide; these grains remained undissolved, but TiC precipitated upon them during solidification.

Supplemented by other structural studies of melted powder mixtures, these preliminary results indicated: (a) the anticipated quasi-binary probably did not exist; (b) oxygen and nitrogen could form dark gray and rose-colored phases in the microstructure in addition to raising the liquidus (inhibiting wetting) and lowering the solidus (indicated by the additional eutectic.) Consequently, the subsequent plan of work was to examine the whole nickel end of the ternary system by a procedure designed to eliminate contamination as much as possible.

## B. Procedure.

### 1. Alloy Preparation:

Compositions were prepared from the following materials:

- (a) blocks cut from a reject ingot of spectroscopic quality nickel containing 99.96 per cent nickel plus cobalt (given

- by International Nickel Company);
- (b) spectroscopic carbon electrodes;
- (c) titanium sponge prepared by du Pont.

In a few cases, mixtures of nickel powder (98.43 per cent nickel plus cobalt) and 19.6 per cent carbon TiC (prepared by Kennametal) were used.

Ingots were arc cast in a nickel-plated, water-cooled copper crucible with a graphite electrode in a closed helium atmosphere, pre-purified through activated charcoal at -187 C and gettered prior to melting each alloy by melting successively several buttons of sponge titanium. This procedure probably confined contamination to that within the starting materials, although minute amounts of oxygen and nitrogen could not be eliminated from the samples.

Each ingot was weighed, sectioned, and examined for homogeneity. Chips were machined from the sectioned surface of one-half of each ingot of critical composition for analysis of carbon and titanium. (See Appendices B through F for the details of alloy preparation and chemical analysis.)

## 2. Heat Treatment:

Each ingot was cut and broken into six or eight wedges, which were placed in pre-reduced zirconia boats for treatment at different temperatures. A zircon tube, heated by globars, constituted the furnace chamber. The helium atmosphere was pre-purified through calcium at 650 C and gettered by titanium sponge placed in the chamber near the samples. The temperature directly above the samples was measured by a platinum - 10 per cent rhodium thermocouple protected by a

glazed porcelain sheath. The thermocouple was calibrated against the melting point of gold and the freezing point of copper, and the temperatures of the samples were checked with those measured by melting wedges of the pure nickel and of electrical copper.

To determine the solidus, the samples were held at different temperatures for 20 to 60 minutes and quenched into water. Such times were more than sufficient to cause solution and coalescence of the as-cast carbide structure at temperatures near the solidus, and the quench transformed any liquid present to an easily identified eutectic structure. Temperature measurement and control was usually accurate to within 3 degrees C, and data for important compositions were re-checked.

The liquidus could not be obtained by this method, since some decarburization and oxidation occurred despite the efforts to purify the atmosphere. Where large amounts of alpha remained solid, however, the decarburized rim at the sample surface was confined to a narrow region, and incipient melting in the interior was not affected.

In addition, the equilibrium with graphite was checked at 1240 and 1190 C by annealing alloys for 24 hours and 10 hours respectively. These times were sufficient for the nucleation and growth of new graphite particles and for the coalescence of most of the carbide eutectic.

Appendices G and H give further details of the heat treatment procedure.

### 3. Examination:

Each treated sample was sectioned and mounted for microscopic examination. Polishing was conducted with diamond dust (Diamet Hyprez) in kerosene on the back of photographic paper and on "Miracloth". Carapella's reagent (acidified  $\text{FeCl}_3$  in alcohol) was used as the etch. Density, hardness, and volume percentages were measured in a few cases to supplement the structure data, and the carbide phase in the microstructures was identified with  $\text{TiC}$  by the spectrometer pattern of a polished surface.

An approximation of the limits of the alpha phase was obtained by a crude magnetic analysis. The Curie point of nickel (353 C) is decreased uniformly with increasing titanium to room temperature at about 10 atomic per cent titanium;<sup>42</sup> data by Kase<sup>15</sup> and Bernier<sup>19</sup> on nickel supersaturated with carbon shows that carbon has a slightly less effect. While the odd shapes of the specimens and the decarburized surfaces prevented accurate Curie point measurements, an approximation of the alpha composition in different specimens could be obtained by immersing the specimens in a liquid bath, which was slowly heated or cooled, and determining the temperature range in which the attraction of the specimens to an alnico magnet decreased to a very low value. While the precision of such a method is inherently low, a good check with the reported Curie point of pure nickel was obtained.

Carbide lattice parameters were compared by the powder method, using a Phragmen camera with iron and copper radiation.

### C. Results.

#### 1. Tentative Diagram Nickel-Titanium-Carbon Above 1200 C:

The quantitative information obtained is presented in terms of a projection onto a 1200 C basal plane (Figure 3) and three vertical sections through the diagram (Figures 4 and 5), plotted on an atomic per cent scale. Table I summarizes the features that have been determined. Appendix D gives the exact alloy compositions.

Accuracy of the eutectic temperatures listed is probably within  $\pm 4$  degrees C; the size of the blocks in Figures 4 and 5 is representative of the maximum error in each measurement, and these figures are reproduced accurately to scale. The eutectic compositions listed in Table I are based on the microstructures of nearby alloys, and these points are very approximate.

Alpha solvus data for compositions having more than 10 atomic per cent titanium could not be obtained, since the magnetic analysis indicated that equilibrium with respect to  $\text{TiNi}_3$  was not achieved at the lower temperatures. The remainder of the solvus was determined, however, using magnetic data from many compositions and the structures in the two alloys richest in nickel. The boundary at 1200 C thus obtained was extrapolated to the nickel-titanium binary.

It is possible that residual oxygen and nitrogen in the alloys caused a shifting of the nickel-rich boundaries to slightly lower carbon contents than would occur in the true ternary system; however, the agreement between the data for different compositions is good, and the colored contaminated phases were not observed in the ternary compositions in this region of the system.

Fig 3 - Nickel-Titanium-Carbon diagram  
projected onto a basal plane at  
1200 C (atomic per cent scale).  
Circles indicate the compositions;  
long-dash lines are on the liquidus;  
short-dash lines are on the solidus.

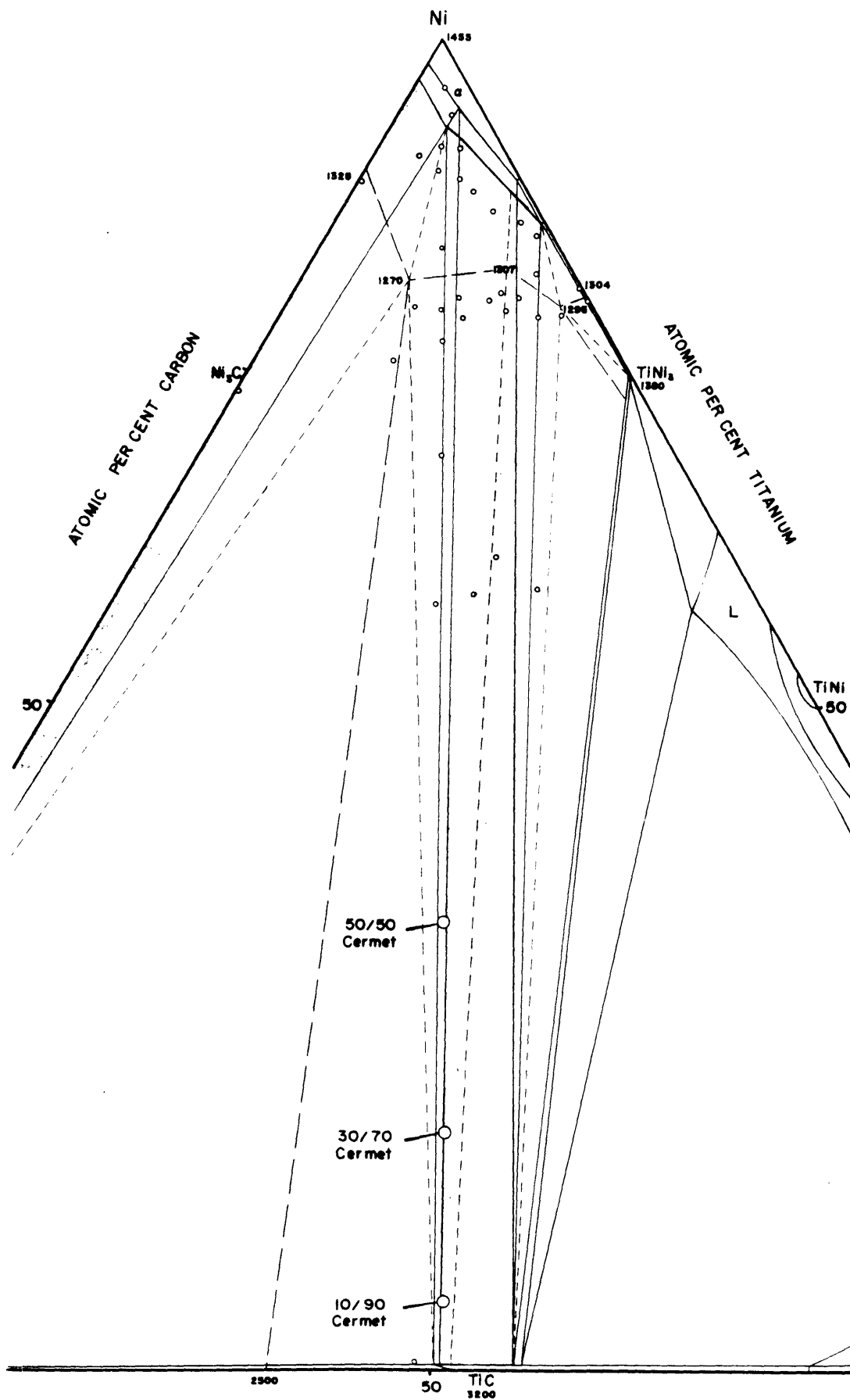


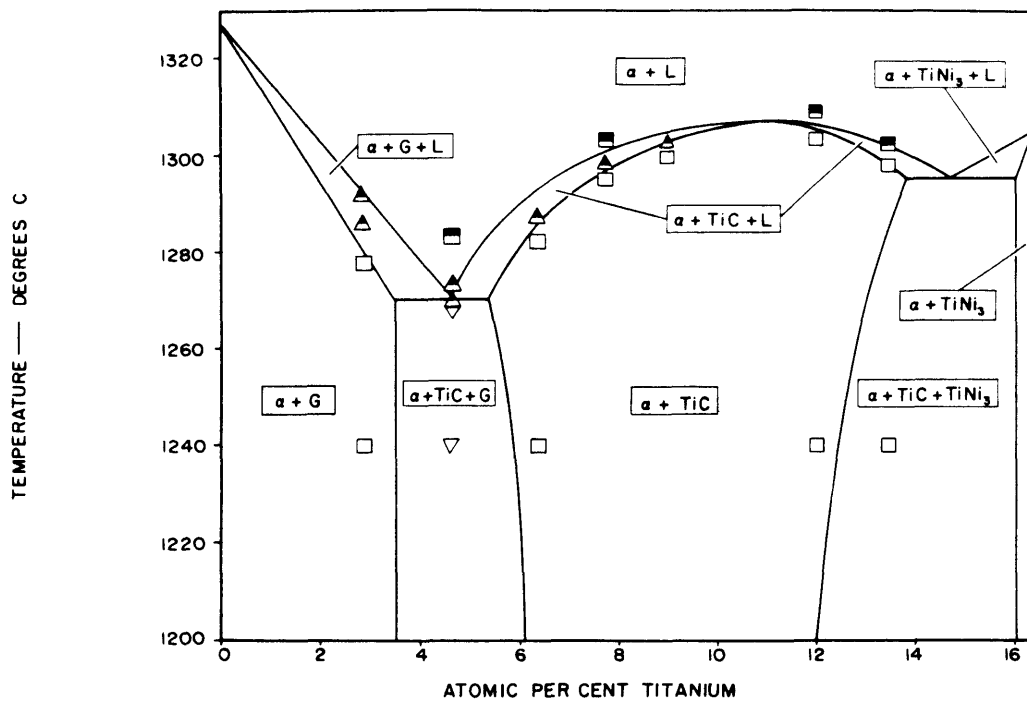


Fig 4 - Vertical sections across the  $\alpha$  + TiC field showing data obtained.

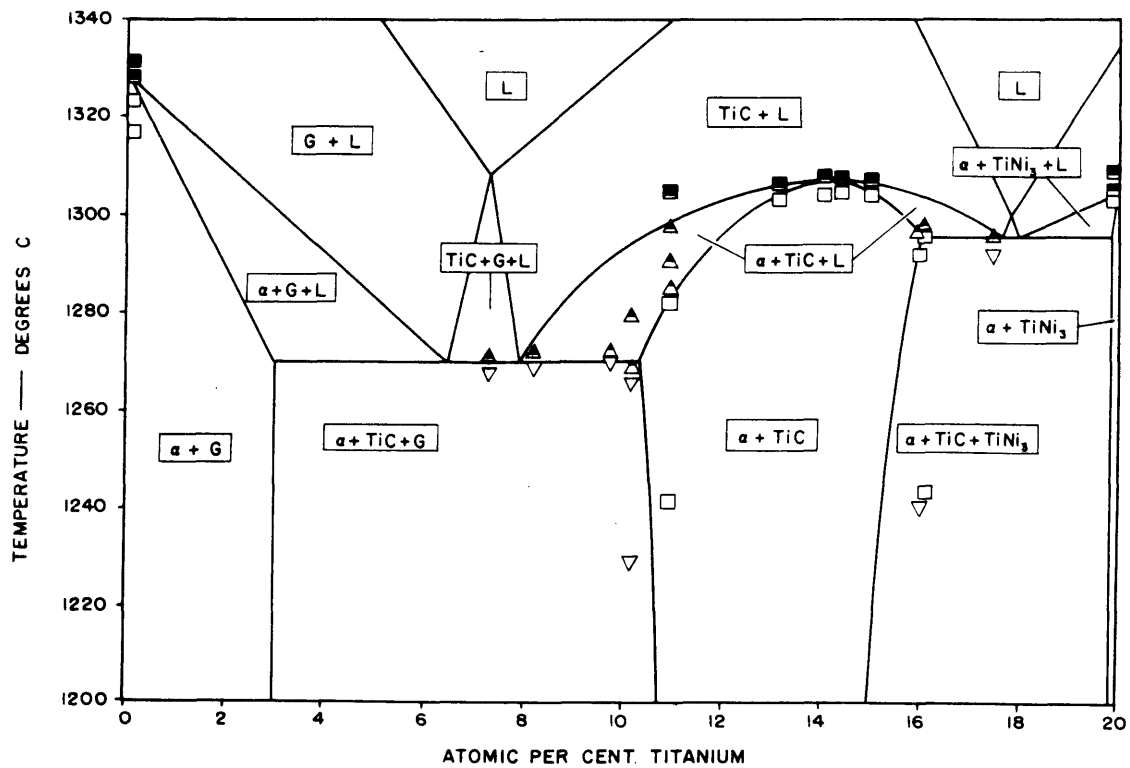
A: Section between 7 atomic per cent carbon, 0 atomic per cent titanium, and 0 atomic per cent carbon, 16.4 atomic per cent titanium.

B: Section between 20 atomic per cent carbon, 0 atomic per cent titanium, and 0 atomic per cent carbon, 20 atomic per cent titanium.

Squares: two-phase fields;  
Triangles: three-phase fields;  
Relative amount of liquid indicated  
by proportion of black.



A



B

Fig 5 - Vertical section between pure  
nickel and commercial TiC  
(49.5 atomic per cent carbon).

Circles: one-phase fields;  
Squares: two-phase fields;  
Triangles: three-phase fields;  
Relative amount of liquid indicated by proportion of black.

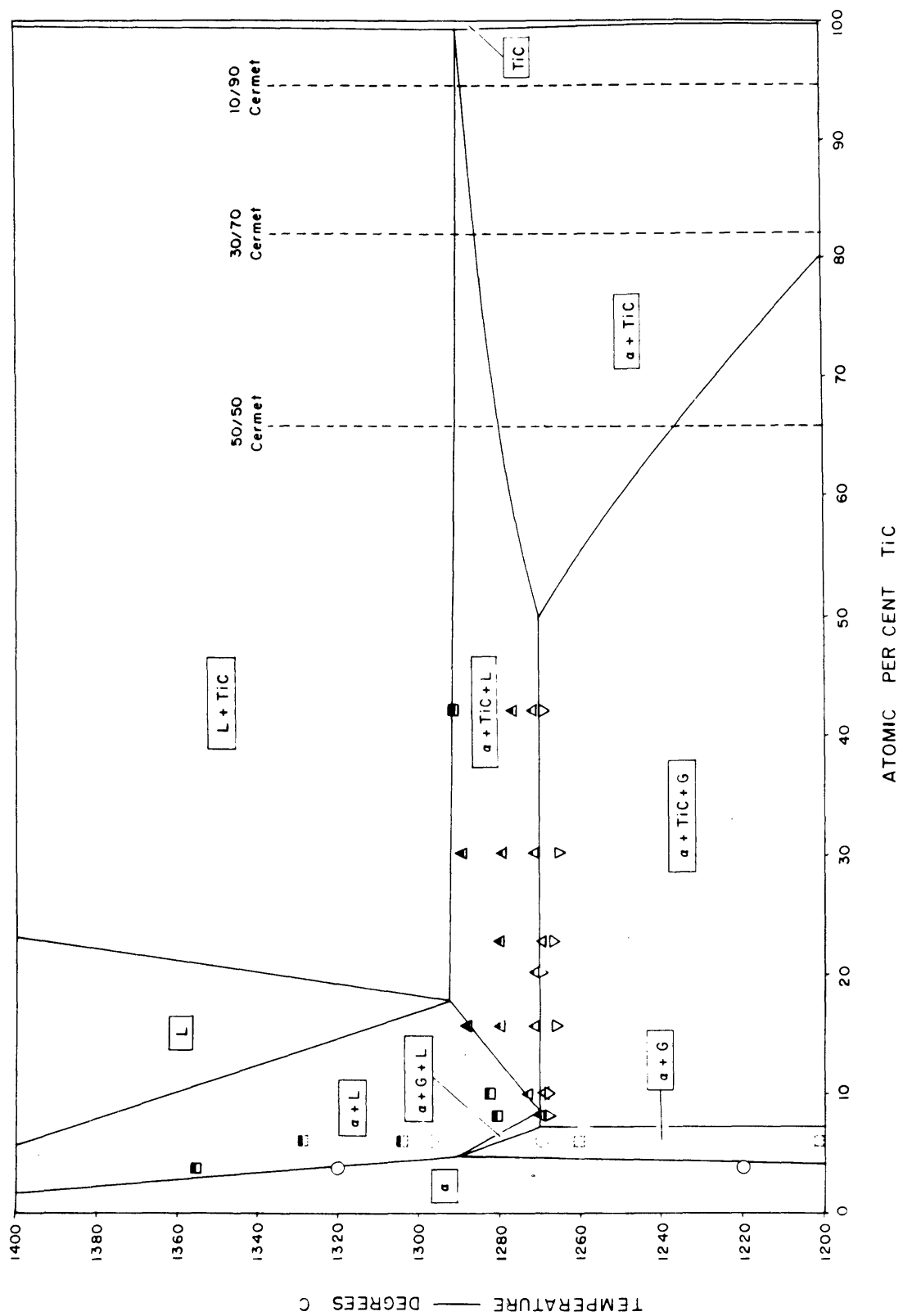


Table I. FEATURES OF THE SYSTEM NICKEL-TITANIUM-CARBON

Feature	Phases	Temperature Degrees C	Atomic Percent C	Atomic Percent Ti	Weight Percent C	Weight Percent Ti
Eutectic	$\frac{L}{\alpha + G}$	1328	10.0	-	2.2	-
Eutectic	$\frac{L}{\alpha + TiC + G}$	1270	11	7	$2\frac{1}{2}$	$6\frac{1}{2}$
Eutectic	$\frac{L}{\alpha + TiC}$	1307	4	13	0.9	11.2
Eutectic	$\frac{L}{\alpha + TiC + TiNi_3}$	1295	$2\frac{1}{2}$	$17\frac{1}{2}$	$\frac{1}{2}$	15
Eutectic	$\frac{L}{\alpha + TiNi_3}$	1304	-	18	-	15
Solvus	$\frac{\alpha}{TiC + G}$	1270	2.8	3.6	0.6	3.0
		1260	2.3	3.6	0.5	3.0
		1200	1.8	3.6	0.4	3.0
Solvus	$\frac{\alpha}{TiC + TiNi_3}$	1295	$\frac{1}{2}$	$13\frac{1}{2}$	0.1	$11\frac{1}{2}$

The limits of the TiC phase in this system were not studied systematically. However, a 30 weight per cent nickel cermet sintered in vacuum at 1350 C for 4 hours was leached electrolytically by the method described by Chang,<sup>43</sup> and the powder obtained was analyzed chemically and by X-rays. The parameter observed was the same as that of the original TiC powder, and the analyzed nickel content was less than 0.05 per cent. An arc-cast composition containing about 0.8 per cent nickel by weight showed considerable free alpha as well as graphite in segregated areas of the microstructure. Thus, the solubility of nickel in TiC appears to be negligible.

The titanium-rich region of the system was not investigated, but diffusion regions obtained in a few castings high in titanium showed that each of the binary intermetallics,  $Ti_2Ni$ ,  $TiNi$ , and  $TiNi_3$ , form two-phase fields with TiC on solidification. Thus, a ternary carbide phase cannot occur in TiC - nickel cermets, unless it forms from the solid state at lower temperatures.

The diagram below 1200 C may have some significance for cermet manufacture since it was found that a vacuum-sintered cermet containing 30 weight per cent nickel had a Curie point very close to that of the nickel powder used in its manufacture. The finely dispersed structure revealed in the binder of commercial cermets at high magnifications was not found in any of the high nickel alloys studied here; but it is possible that stresses resulting from differential contraction between the carbide and alpha phases induce precipitation at very low temperatures during furnace cooling, thus resulting in a low alloy

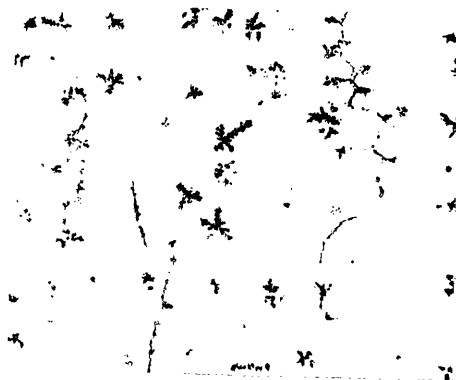
content in the binder. The precipitation in Figure 2-A may illustrate such an effect.

## 2. Phase Shape and Mode of Formation:

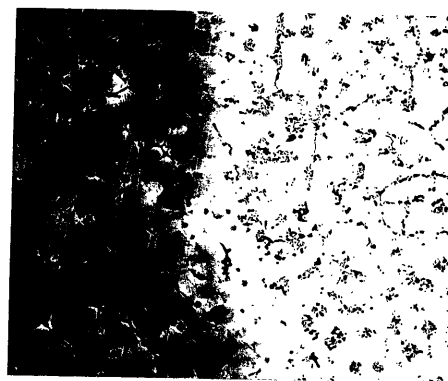
The mechanical properties of cermets are influenced by the size, shape, and distribution of the grains. Small, rounded, uniformly distributed carbide grains have been associated with higher strengths than the large, angular grains resulting from sintering at high temperatures. Large graphite plates in the microstructure have been blamed for weakness in some cases, although small amounts of finely distributed graphite does not appear to cause much damage.<sup>2</sup> Thus, information regarding the nucleation and growth of the phases on cooling from the sintering temperature is just as important as the equilibrium relationships.

Figures 6, 7, and 8 illustrate the most informative microstructures encountered. The pictures were taken of etched samples under polarized light. Together, they provide a picture of the grain formation under the conditions of non-equilibrium solidification which may be encountered in commercial sintering practice.

Primary TiC, solidified rapidly from large amounts of liquid, always develops sharp crystals of cubic symmetry (Figure 7 A, B, and E). The corners can be rounded by solution and reprecipitation through solid alpha by short anneals within 5 to 10 degrees of the solidus (Figure 8 A, and E). High carbide compositions, in which solidification occurs at higher temperatures and is accompanied by a greater evolution of heat, form rounded dendrites directly on arc casting



(A): 10.5 at-O / 89.5 at-Ni as cast.  
Approximately eutectic composition.  
Hardness - Rockwell B 85. —200X.



(B): Same as (A) annealed at 1328 °C and  
water quenched. Unmelted top of sample  
at right. Hardness at left - Rockwell  
B 82; at right - B 60 - 65. —100X.



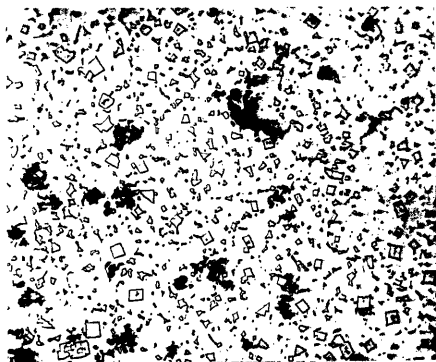
(C): 18.5 at-Ti / 81.5 at-Ni as cast.  
Approximately eutectic composition.  
Primary  $TiNi_3$  plates in eutectic matrix.  
A few tiny particles of yellow TiN.  
—225X.



(D): TiO - graphite eutectic in an arc cast TiO  
block. Approximately 17 pct graphite by  
volume. Unetched. —500X.

Fig 6 - Important binary microstructures (reduced one-half)





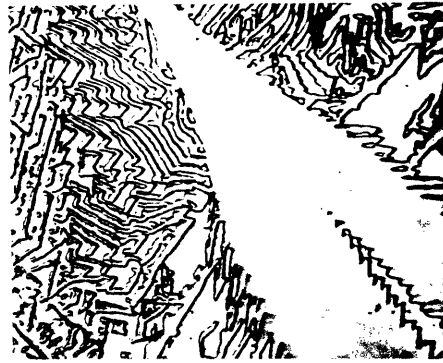
(A): 11.8 at-C / 8.4 at-Ti / bal Ni as cast.  
Close to ternary eutectic composition.  
( $\alpha$  + TiC + G) —750X.



(B): 15.3 at-C / 8.8 at-Ti / bal Ni as cast.  
Primary graphite and TiC in a matrix of  
carbide eutectic, supercooled graphite,  
and alpha dendrites. —750X.



(C): Same as (B). Alpha + TiC eutectic  
structure. —1600X.



(D): Same as (B). Rapidly cooled carbide grain  
and eutectic near crucible wall. —1600X.

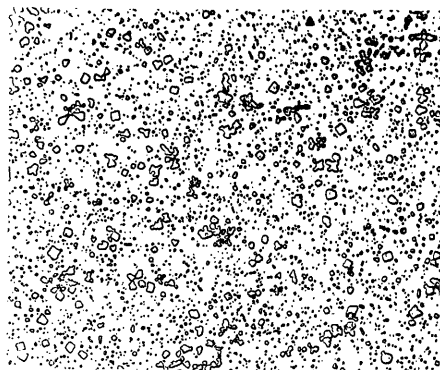


(E): Same as (B). Typical graphite spherulite  
surrounded by plates. Note carbide and  
graphite precipitate from alpha within  
carbide grain. —1000X.



(F): TiC - nickel powder mixture of approximate  
cermet composition as cast. Note carbide  
precipitate from alpha and absence of graphite.  
—500X.

**Fig 7 - Important as-cast microstructures (reduced one-half)**



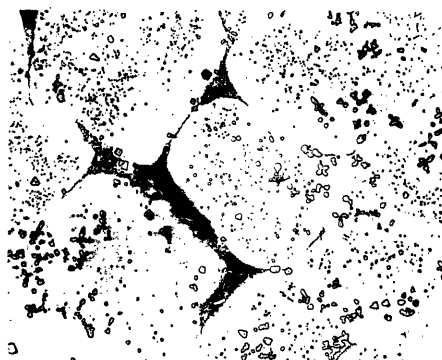
(A): 5.6 at-% / 13.3 at-% Ti / bal Ni annealed at 1305 °C. Close to quasi-binary eutectic composition. Solution and coalescence of eutectic structure. ( $\alpha$  + TiO). —250X.



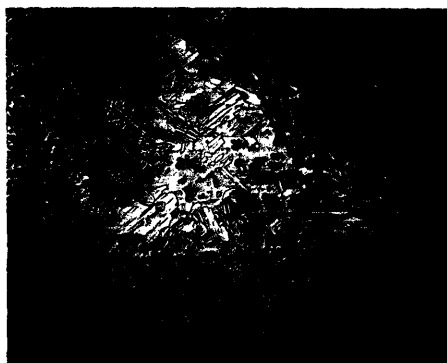
(B): Same as (A) annealed at 1308 °C and water quenched. Note undissolved carbide floating to top of sample at right and solidification of liquid as alpha dendrites and eutectic. ( $\alpha$  + TiO). —250X.



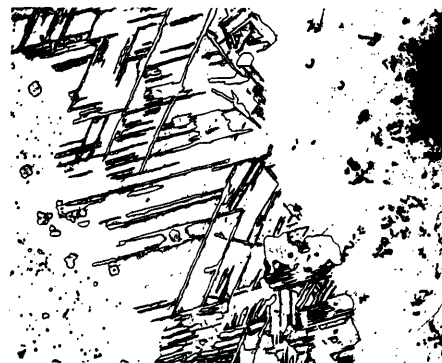
(C): 6.0 at-% / 2.9 at-% Ti / bal Ni annealed at 1295 °C and water quenched. Liquid has solidified as supercooled graphite and anisotropic carbide eutectic. ( $\alpha$  + G + L). —300X.



(D): 2.6 at-% / 14.9 at-% Ti / bal Ni annealed at 1296 °C and water quenched. Liquid has solidified as TiNi<sub>3</sub> and anisotropic carbide eutectic. ( $\alpha$  + TiO + L). —300X.



(E): 2.8 at-% / 17.8 at-% Ti / bal Ni annealed at 1284 °C and water quenched. Small plates of TiNi<sub>3</sub> embedded in alpha dendrites and coalesced TiO. ( $\alpha$  + TiO + TiNi<sub>3</sub>). —300X.



(F): 4.0 at-% / 15.6 at-% Ti / bal Ni annealed at 1280 °C. Decarburized and detitanized rim due to unusually impure atmosphere; original ( $\alpha$  + TiO) structure at left, oxide at right. —300X.

Fig 8 - Important annealed microstructures (reduced one-half)

(Figures 6 D and 7 F). Contaminated microstructures (not shown) indicate that TiC is nucleated by the colored oxygen- and nitrogen-rich phases, and that more of a tendency to develop rounded grains exists when these elements are in solution.

The first primary graphite to solidify frequently was sperulitic in structure, but surrounding regions formed plate graphite on further solidification (Figure 7 B and E.) Although graphite - TiC interfaces frequently occurred, no predominating tendency for TiC to nucleate graphite from the liquid could be noticed. Secondary graphite in the TiC-graphite eutectic is plate-like in nature (Figure 6 D.).

TiNi<sub>3</sub>, the only intermetallic which could be involved in ternary cermets, occurs as large plates, when formed from either the liquid (Figures 6 C and 8 E) or solid alpha (Figure 8 F). Since it did not form readily from the solid upon annealing at low temperatures, even after moderate cold work, the nucleation rate must be quite low at the lower temperatures.

The alpha binder is the last phase to solidify in commercial compositions. If the cooling rate is sufficiently rapid, this phase can become supersaturated in both carbon (Figure 6 A and B) and titanium (indicated by a lower Curie point in cast binary samples than in those quenched from the solidus). The solubility in alpha of TiC plus graphite is displaced to slightly higher carbon contents by rapid cooling, since less graphite was found in the structure formed from the liquid in compositions cast or water-quenched than in the same alloys annealed at the solidus.

Although primary TiC tends to nucleate alpha during solidification (Figure 7 B and 8 B), the nucleation of TiC is sufficiently

inhibited by rapid cooling to cause a quasi-eutectic structure (Figure 7 C) to form at some low temperature, possibly characteristic of spontaneous carbide nucleation. The eutectic composition is suppressed to higher carbide contents than the equilibrium composition, resulting in primary alpha dendrites in the microstructure (Figure 8 B and 9 B). The size and separation of the eutectic plates decreases with increasing cooling rates and with decreasing carbon content across the two-phase field (alpha plus TiC). The eutectic structure did not occur where the solidifying binder was largely surrounded by primary carbide (Figure 7 E and F) and in one high-nickel composition (Figure 7 A), in which solidification was confined to a narrower range of temperature.

A eutectic structure of another carbide phase formed from water-quenched liquid of two compositions with carbon - titanium ratios far from that of TiC (Figure 8 C and D). This structure, finer and softer than the TiC eutectic, shows a definite anisotropy under polarized light, whereas TiC and the contaminated "pink" eutectic do not. A non-equilibrium structure, this carbide may be related to  $\text{Ni}_3\text{C}$ . Such a carbide was not found in the binary compositions, although the presence in the cast eutectic alloy (Figure 6 A and B) of supersaturated " $\text{Ni}_4\text{C}$ " and graphite dendrites resembling temper carbon suggest its transient existence.

#### IV. DISCUSSION AND CONCLUSIONS

##### A. The Equilibrium Diagram.

The portion of the ternary system studied here is of a simple type, possessing a "quasi-binary eutectic" between the alpha and carbide phases. However, since the substitutional solubility of titanium in nickel is about four times the interstitial solubility for carbon, this "quasi-binary" is pulled away from the section between the component and the compound. The other ternary systems between cobalt or nickel and the carbides of transition elements of groups IV and V probably show this same feature, since the binaries are similar. It may be a general feature of all carbide-metal cermets that liquid and solid binder are at equilibrium over a range of temperatures, in contrast to the idea of a "eutectic" which has been presented in the past.

The useful region of the ternary system is summarized in the weight per cent vertical sections of Figure 9, which cover the range of compositions which should be encountered in commercial cermets. Since uncontaminated titanium carbide does not appear to dissolve the stoichiometric amount of carbon, graphite is included throughout the top section of Figure 9. This section might also correspond to cermets prepared from a carbide of lower carbon content, since the oxygen and nitrogen impurities present would tend to displace carbon from interstitial solution in the form of graphite. If sintering is carried out in a high vacuum, however, the formation and removal of carbon monoxide from the compact will cause some decarburization, and free graphite will not form on solidification. The central section of Figure 9 then might correspond

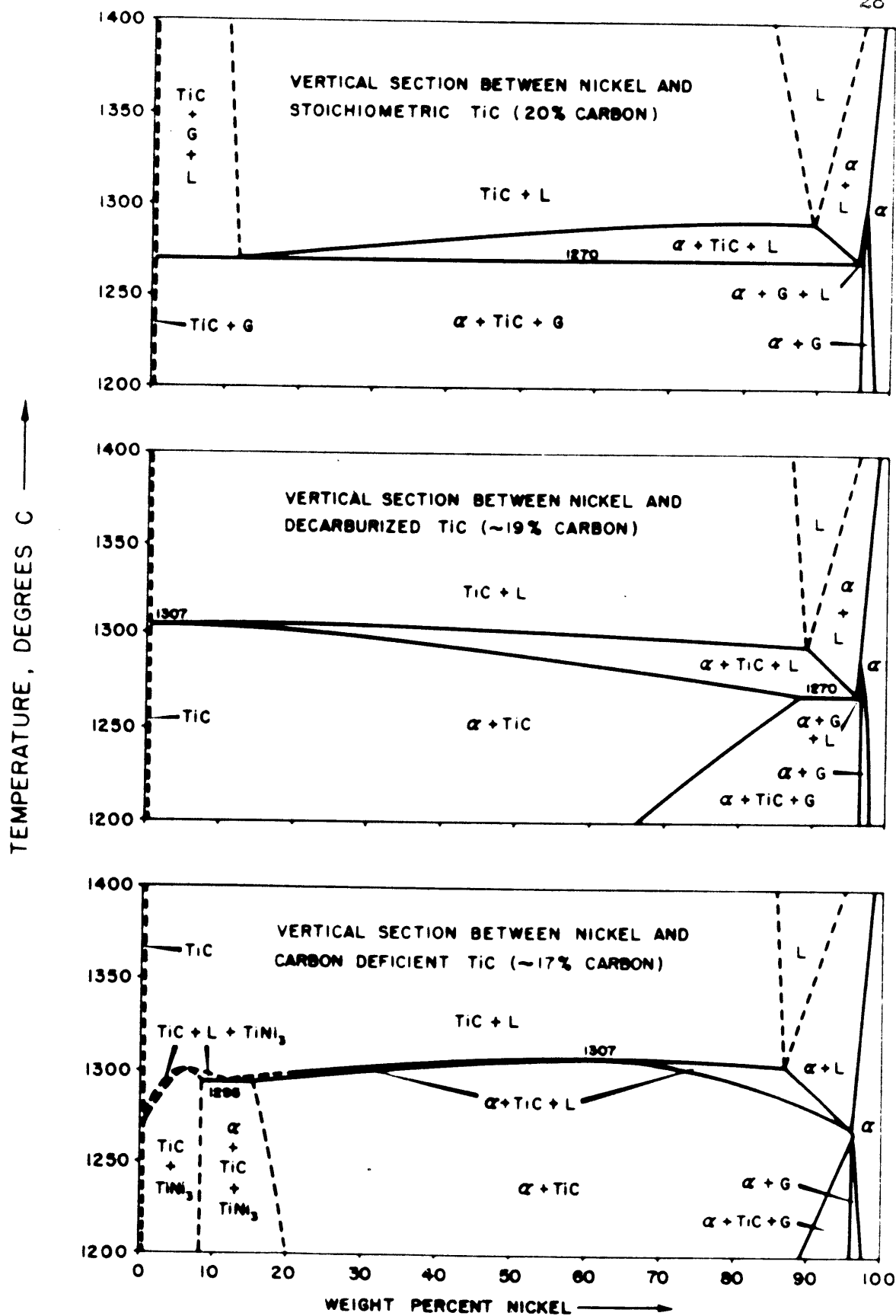


FIGURE 9. VERTICAL SECTIONS THROUGH TERNARY Ni-Ti-C DIAGRAM AT AND NEAR THE TiC-Ni PLANE.

to vacuum-sintered cermets. Note that it is possible to sinter commercial compositions (20 to 60 per cent nickel) in the presence of both liquid and solid binder, but that the width of temperature range for such a treatment decreases with either decreasing nickel or decreasing carbon in the alloy.

In small amounts, the effect of the impurities and addition agents normally found in commercial cermets may be expressed with the aid of the equilibrium diagram. Oxygen and nitrogen can effectively increase the carbon content of a composition by displacing carbon from interstitial solution in both alpha and TiC. Transition metal impurities or additions shift a composition towards some point on the nickel-titanium binary, the position of that point depending on the valence of the metal. Most impurities or addition elements probably lower the solidus surface of the system and increase the range of the three-phase field (alpha plus carbide plus liquid), carbon being constant.

#### B. Binder Phase Relationships during Sintering.

The phase changes that take place during sintering can best be reviewed by the history of a cermet body.

When the pressed compact is first heated, liquid will be in equilibrium at 1270 C due to the free carbon in the carbide powder. However, the presence of oxide films around the carbide grains will inhibit solid state diffusion, and liquification may be suppressed to a higher temperature, perhaps in the range of the nickel-graphite eutectic. All of the binder will be liquid at equilibrium above the range 1290 to 1305 C. In this temperature region, or slightly above it, carbon and

oxygen in the sample will react to produce carbon monoxide, which can form large bubbles trapped within the compact if sintering is not carried out in a sufficiently high vacuum.

At a sintering temperature of 1350 C, about one-third of the volume of a 40 weight per cent nickel cermet should be liquid, assuming a liquid density of 7.9 grams per cubic centimeter. While the total amount of liquid present does not increase rapidly with increasing temperature (the liquidus for this composition is probably above 2500 C), an increased rate of carbide grain growth, by solution and redeposition through the liquid, will result in a larger volume of liquid around each carbide grain at the higher sintering temperatures. Rapid cooling from such temperatures causes larger, more angular grains to form in the cermet microstructure. If the temperature is kept sufficiently low, on the other hand, solution and redeposition will occur without much total grain growth, and small, rounded or kidney-shaped grains will result. The best sintering temperature and time will be a balance between that required to remove all of the carbon monoxide produced by solution of the impure carbide, and that necessary to retain a small, uniform grain size.

Upon cooling from the sintering temperature, carbide will deposit on all primary grains, even those which might not have dissolved at all during sintering due to the presence of contaminated surface layers. The alpha phase will solidify over a small range of temperatures, while the eutectic carbide continues to deposit on the primary. The composition of both the liquid and the alpha in equilibrium with



the liquid will increase in carbon and decreases in titanium with decreasing temperatures. Although graphite plates would tend to precipitate from the last liquid to solidify, the rapid rate of solid diffusion near the solidus, together with the tendency for the binder to become supersaturated in carbon upon rapid cooling, should eliminate such precipitation if the carbon and oxygen contents have been sufficiently reduced by high vacuum sintering. The higher the nickel content of a cermet, the greater will be its tendency to form graphite, as illustrated in Figure 9.

At very low temperatures, the stresses in the binder set up due to the difference in contraction between the carbide and alpha phases may induce precipitation of finely distributed carbide, graphite, or some transition structure, leaving behind the pure and ductile binder necessary for toughness and strength in cemented carbides.

## V. SUMMARY

The nickel-rich portion of the system nickel-titanium-carbon has been tentatively determined above 1200 C by metallographic examination of samples quenched from different temperatures, supplemented by thermal analysis and magnetic, X-ray and density measurements. The equilibrium surfaces thus obtained, together with modifications of the phase boundaries and grain structure due to non-equilibrium solidification and oxygen and nitrogen contamination, allow a detailed discussion of the role of the binder in sintering titanium carbide - nickel cermets.

## VI. BIBLIOGRAPHY

1. W. J. Engel: Bonding Investigation of Titanium Carbide With Various Elements, NACA Technical Note 2187, Sept. 1950.
2. E. M. Trent, A. Carter, J. Bateman: High Temperature Alloys Based on Titanium Carbide, Metallurgia (1950) 42, pp 111 - 115.
3. R. G. Bourdeau: Titanium Carbide Cemented With Nickel, SB Thesis, Mechanical Engineering Dept., M.I.T., 1951.
4. Polikarpova: Extract of paper submitted to obtain degree of Certified Engineer, MGU, 1937, X-Ray Laboratory, Elektrozavode. Quoted by G. A. Meerson, et al in reference 39; Butcher Translation 1642, p 5.
5. N. M. Zarubin and L. P. Molkov: Investigations of Alloys Produced According to Ceramic Methods, Vestnik Metalloprovo (1935) 15, pp 93 - 98; Chemical Abstracts 31, 6170.
6. N. M. Zarubin and R. A. Trubnikov: On the Study of the State Diagram of the Systems Carbide-Chromium-Cobalt and Carbide-Chromium-Nickel, Redki Metali (1935) No. 2, p 38.
7. S. Takeda: A Metallographic Study of the Action of the Cementing Materials for Cemented Tungsten Carbide, Science Reports Tohoku Imperial University, First Series, Honda Anniversary Volume (1936), p. 864.
8. P. Rautala: The Wolfram-Carbon-Cobalt System, ScD Thesis, Metallurgy Department, M.I.T., 1951.
9. \_\_\_\_\_: Determination of the Solid Solubility of Cobalt and Iron in Refractory Carbides, Studiengesellschaft Hartmetall, Feb, 1941; US Dept. of Commerce PB 100652 (BOT FD 3864/47); also abstracted in Metal Powder Report, May, 1948, p 142.
10. R. Kieffer: Theoretical Aspects of Sintering of Carbides, The Physics of Powder Metallurgy (edited by W. E. Kingston), McGraw-Hill, 1951, pp 278, - 291.
11. A. G. Metcalfe: The Mutual Solid Solubility of WC and TiC, Jnl Inst of Metals (1947) 73, p 591.
12. T. E. Kihlgren and J. T. Eash: Carbon-Nickel, ASM Metals Handbook, American Society for Metals, 1948, p 1183.
13. V. K. Kriedrich and A. Leroux: Information on the Melting-Point Diagram of Nickel-Carbon Alloys, Metallurgie (1910) 7, pp 10 - 13.

14. O. Ruff and W. Bormann: Studies in the Range of Higher Temperatures VI: Nickel and Carbon, Zeitschrift für Anorganisch Chemie (1914) 88, pp 386 - 396.
15. T. Kase: On the Equilibrium Diagram of the Iron-Carbon-Nickel System, Science Reports of the Tohoku Imperial University (1925) 14, pp 174 - 217.
16. H. Morrogh and W. J. Williams: Graphite Formation in Cast Irons and in Nickel-Carbon and Cobalt-Carbon Alloys, Jnl Iron and Steel Inst (1947) 155, pp 322 - 369.
17. J. E. Hofer, E. M. Cohn, and W. C. Peebles: Isothermal Decomposition of Nickel Carbide, Jnl Physical and Colloid Chemistry (1950) 54, pp 1161 - 1169.
18. R. Bernier: Thermomagnetic Studies of the Carbides of Iron and Nickel, Annales de Chimie (Jan-Feb, 1951) 6, pp 104 - 161.
19. J. P. Nielsen (New York University): Nickel-Titanium diagram presented at the Fourth Conference on Titanium, Wright-Patterson Air Field, Jan. 24 - 25, 1952.
20. W. Rostoker: Observations on the Occurrence of  $Ti_2X$  Phases, Trans AIME, Jnl of Metals (1952) 4, pp 209 - 210.
21. V. F. Laves and H. J. Wallbaum: The Crystal Chemistry of Titanium Alloys, Naturwissenschaften (1939) 27, pp 674 - 675.
22. V. F. Laves and H. J. Wallbaum: The Crystal Structure of  $Ni_3Ti$  and  $Si_2Ti$  (Two New Types), Zeitschrift für Kristallographie, (1939) A101, p 78.
23. E. N. Skinner: Nickel-Titanium, ASM Metals Handbook, American Society for Metals, 1948, p 1235.
24. R. Vogel and H. J. Wallbaum: The System Iron-Nickel- $Ni_3Ti$ - $Fe_2Ti$ , Archive für das Eisenhüttenwesen (1938) 12, pp 299 - 305.
25. J. P. Nielsen: Titanium-Carbon and Titanium-Nitrogen Alloys, Final Report for the period 1 Dec 1949 to 30 Sept 1950, WAL 401/14 - 12, Contract DA 30-069-GRD 6, Nov 30, 1950.
26. J. G. McMullin: The Constitution of Titanium-Tantalum-Carbon Alloys, Metallurgy Dept, MIT, 1952; also thesis by D. V. Ragone, SE, 1951, and G. W. P. Rengstorff, SM, 1948.
27. P. Ehrlich: On the Binary Systems of Titanium with the Elements Nitrogen, Carbon, Boron, and Beryllium, Zeitschrift für Anorganisch Chemie (1949) 259, pp 22-41; Butcher Translations 2598 and 2599.

28. J. P. Nielsen (New York University): personal communication to J. G. McMullin (MIT), February, 1952.
29. R. Kieffer and F. Kolbl: International Powder Metallurgy Conference, Graz, Austria, July 12-17, 1948, Ref No 28; quoted by C. G. Goetzel in Treatise on Powder Metallurgy, Vol II, New York, 1950, p 83.
30. F. W. Glaser and W. Ivanick: Sintered Titanium Carbide, Trans AIME, Jnl of Metals (1952) 4, pp 387-390; See also patents by H. R. Montgomery: US 2,496,671, and C. C. Laughton and E. Wainer: US 2,491,410.
31. A. N. Zelikman and N. N. Gorovits: Study of Interaction between Nitrogen and Titanium Carbide, Zhurnal Prikladnoi Khimii (1950) 23, pp 689-695; Brutcher Translation 2593.
32. G. A. Meerson and Y. M. Lipkes: Investigation of the Conditions of Titanium Carburization III and IV, Zhurnal Prikladnoi Khimii (1945) 18, pp 24-34 and 251-258; Brutcher Translations 928 and 2567.
33. K. Becker: High Melting Hardmetals and their Technical Manufacture, Berlin, 1935, p 57.
34. H. Krainer: Physical Studies of Titanium Carbide and of Cemented Carbide Compositions Containing Titanium Carbide, Archive für das Eisenhüttenwesen (1950) 21, pp 123-127; Brutcher Translation 2620.
35. C. G. Goetzel: Treatise on Powder Metallurgy, Vol II, New York, 1950, p 81.
36. P. Duwez and F. Odell: Phase Relationships in the Binary Systems of Nitrides and Carbides of Zirconium, Columbium, Titanium, and Vanadium, Jnl Electrochemical Society (1950) 97, p 299.
37. Armour Research Foundation: Titanium Phase Diagrams, Report No. 9, for Air Materiel Command, Wright-Patterson Air Force Base, June 11, 1951, p 13.
38. I. S. Gaev: Diffusion of Titanium and Dissociation of Titanium Compounds, Metallurg (1934) 9, pp 19-33; Brutcher Translation 940.
39. G. A. Meerson, G. L. Zverev, and B. Y. Osinovskaya: Investigation of Behavior of Titanium Carbide in Cemented Carbide Alloys, Zhurnal Prikladnoi Khimii (1940) 13, pp 66-75; Brutcher Translation 1642.
40. F. H. Pollard and P. Woodward: The Stability and Chemical Reactivity of TiN and TiC, Trans of the Faraday Society (1950) 46, pp 190-199.

41. J. P. Nielsen and H. Margolin: Titanium Nickel Phase Diagram, Summary Report, Dec 1, 1950, for contract AF 33(038)-8725, Research Division, New York University, Fig 9, plate VII.
42. R. M. Bozorth: Ferromagnetism, Van Nostrand, 1951, p 325.
43. L. C. Chang: Discussion on the Isolation of Carbides from High Speed Steel, by D. J. Blickwede and M. Cohen, Trans AIME (1950) 188, p 1061.

## VII. SUGGESTIONS FOR FURTHER RESEARCH

Future work on this subject which might be the most profitable may be along the following lines:

Nickel-rich portion of the diagram: An accurate study of the alpha solvus surface, perhaps accompanied by an identification of the binder precipitate in cermet, could be made by preparing high purity solid solution compositions, completely free of oxygen and nitrogen, and obtaining accurate Curie point measurements and lattice parameters, after working and annealing samples down to very low temperatures. The solidus surface of the system, including the two binary eutectics, may also be modified by more accurate work using iodide titanium and vacuum-melted nickel in preparing compositions.

Carbide-rich portion of the diagram: An accurate determination of the TiC solidus and the TiC - graphite solvus might be obtained by arc casting high-purity TiC and annealing samples either by resistance or by radiation from a tungsten shield prior to quenching and examination. The solubility of nickel in TiC might be obtained by careful leaching of completely recrystallized carbide grains from fine-grained compacts, and analyzing the carbide chemically and by X-rays. The effects of oxygen and nitrogen on the equilibrium surfaces and physical properties of the TiC phase should be of such practical interest, that these effects will undoubtedly be subjects of investigation in the near future.

Casting cermets: The manufacture of pure carbides and cermet compositions by arc casting and subsequent heat treatment should be studied, since such a method provides a means of obtaining a completely dense material with a minimum of effort. As shown in Figure 7 F, kidney-shaped grains can be produced in cermet compositions by arc casting. The principal problems to be solved in such a process are: control of composition, control of grain size, prevention of cracking due to thermal shock on cooling, subsequent shaping of the ingot, and the very high power requirements in casting. Casting carbides and cermets is probably impossible in any refractory container, due to oxygen absorption into the alloy, but graphite molds may be useful if the inevitable free graphite in the microstructure can be rendered harmless.



## VIII. APPENDIX

### A. Thermal Analysis.

#### 1. Procedure:

The principal experiments were carried out in the apparatus described by Zillman.\* Pressed powder compacts were packed into a zirconia crucible, 1-1/4 inches inside diameter by 2-7/8 inches deep, around a zirconia shield, 1/2 inch outside diameter, 3/8 inch inside diameter, and 2 inches deep. The crucible was placed inside a graphite sleeve, which was heated by induction from a copper coil, about 6 inches in diameter and 4 inches high; a longer coil would have produced a more uniform temperature in the sample, but power limitations prevented such a modification. The graphite sleeve was surrounded by alundum-plated and coarse zirconia chips, packed into the water-cooled vycore cylinder (closed at one end), which was used as the furnace chamber.

An atmosphere of argon, partially purified by passing through titanium sponge at about 600 C, was supplied by evacuating the chamber with a mechanical pump, and then letting in the gas until a slight positive pressure was achieved. The argon contained about 0.1 per cent nitrogen, which was not completely removed, and oxygen was undoubtedly released by the zirconia refractory, which blackened during use.

The temperature was measured by a platinum - 10 per cent

---

\* R. W. Zillman, Sc.D. Thesis, Metallurgy Department, M.I.T., 1950.

rhodium thermocouple, fitted into an alundum insulator ground to fit inside a 1/4 inch outside diameter clear silica tube. The tube was inserted into the zirconia shield from a rubber seal at the top of the furnace assembly. Whenever the thermocouple wires were not completely protected from the furnace atmosphere, the thermocouple always broke during service. An ice water cold junction was used, and temperatures were recorded every 10 or 20 seconds by reading the millivoltages on a Brown potentiometer.

Power was supplied by a low frequency Tocco induction unit. All attempts to use high frequency produced induced current in the thermocouple. No measurable effect on the temperature measurement resulted from using the Tocco.

The procedure followed was to heat the sample to 1400 - 1500 C under a setting of about 6 KV, and then reducing the setting to about 2 KV. The temperature-time curve resulting was straight and linear through the liquid or solid regions, until a temperature characteristic of the final setting was reached, at which a leveling-off occurred. Solidification usually occurred over a period of 10 to 15 minutes, and since the region of the curve corresponding to this period was also straight, an approximation of the limits of region of solidification was obtained by the intersections of the straight-line portions of the curve.

An attempt was made to utilize a smaller globar furnace, in which the cooling rate could be controlled over a wider range, but the constant temperature region was not sufficiently great in this assembly to warrant continued experimentation.

## 2. Results.

The data obtained is summarized in Table II . Note that there is good agreement between the cooling curves and heating curves made on previously melted ingots in the larger assembly, but that the initial melting of the powder mixtures took place at a higher temperature range. Kennametal TiC was used for the 13.7 and 10 per cent samples, and a poorer grade was used in the 19.0 per cent run. Sugar charcoal was used for the nickel-graphite comparison runs.

Table II. - DATA FROM THERMAL ANALYSIS

Sample Composition	Rate Degrees-C/minute		Degrees C, Measured Temperature	
	Initial	Final	First Inflection	Solidification Region (Extrapolated)
19.0-TiC <sup>*</sup>	H: 33 C: 21	33	1290 1298	1282 - 1327 - 1298
13.7-TiC <sup>*</sup>	C: 14 H: 27 C: 20 H: 30 C: 26	14 27 14 22 18	1290  1307 1232 1278	- 1298 - 1299 1243 - 1290 1245 - 1268 1241 - 1290
10.0-TiC <sup>*</sup>	H: 45 C: 24	41 16	1282	1295 - 1334 1240 - 1287
8.0-C <sup>*</sup>	C: 45	41	1327	1304 - 1314
3.0-C <sup>"</sup>	C: 40 H: 10 C: 11 C: 2	70 15 15 9	1307 (1324 hold) (1311 hold) (1311 hold)	1288 - 1307 1316 - 1328 1294 - 1315 1300 - 1318

(H: - heating)    \* - 300 gm melts in induction furnace.  
 (C: - cooling)    " - 40 gm melts in glowbar furnace.

B. Description of Starting Materials.1. Nickel:

a. Scrap ingot No. 19677 from International Nickel Company.

(1) Quantitative analysis: Weight Pct

Ni + Co :	99.96
Si :	0.003
C :	0.014

(2) Spectroscopic analysis:

Co :	slight trace
Al, Cu, Fe, Mg, Si :	very slight trace
B, Ca :	less than very slight trace

b. Nickel powder lot No. 497-S from Metals Disintegrating Company.

Quantitative analysis: Weight Pct

Ni:	97.65
Co:	0.78
Fe:	0.52
Ca:	0.15
Si:	0.10
Remainder:	0.80

2. Carbon:

Cenco spectrographic electrodes, certified grade.

Spectroscopic analysis:

Cu, Fe, Mg:	very slight trace
-------------	-------------------

3. Titanium:

Vacuum-distilled sponge from du Pont.

Not analyzed, but such sponge is normally 99.5 pct pure.

4. Titanium Carbide:

## a. TiC from Norton Abrasives Co.

(1) <u>Quantitative Analysis</u> (98.8 pct pure):	<u>Weight Pct</u>
Ti :	80.30 (80.16)
C Total:	18.68 (18.71)
C free :	<u>0.19</u>
C combined (by difference):	18.49
Si :	( 0.09)

(2) Spectroscopic Analysis:

<u>Si</u> , <u>Tl</u> , Fe :	0.1 - 0.001 pct
<u>Cr</u> , Al, Ca, Cu, K, Mg, Ni, P, Rb,	
Pb, Sb, Sn, V, Zn, Ag:	0.01 pct or less

## b. TiC from Kennametal Incorporated.

(1) <u>Quantitative Analysis</u> (98.3 pct pure):	<u>Pct</u>
Ti :	79.22
C total:	19.66
C free:	<u>0.60</u>
C combined (by difference):	19.06

(2) Spectroscopic Analysis:

<u>Cr</u> , <u>V</u> , Fe:	1.0 - 0.01 pct
Tl:	0.1 - 0.001 pct
<u>Mn</u> , Ag, Al, Ca, Cu, Mg, Ni, P,	
Rb, Sb, Si, Sn, W, Zn:	0.01 pct or less

### C. Arc Melting Equipment and Procedure.

#### 1. Equipment:

Figure 10 illustrates the melting chamber used in making most of the alloys. Originally constructed and described by J. H. Johnston,\* the apparatus was modified slightly for the present experiments.

Similar in design to the copper crucible arc furnace used in casting titanium-rich alloys, this equipment had several basic features:

a. Crucible: A 1/4 inch thick electrical copper plate, containing three cupped indentations, was given a light nickel plate and bolted over a water circulating chamber.

b. Electrode: A 3/16 inch spectroscopic carbon electrode mounted in a chuck at the base of a water-cooled copper column was used for low melting compositions; a large electrode ground from a 1-inch rod of Acheson graphite (shown at the right in Figure 9) was necessary for high carbide compositions.

c. Shield: A radiation shield of nickel sheet (shown at the left in Figure 9) was placed around the crucible during melting to protect the walls of the chamber from spattered metal.

d. Chamber: an 8-inch diameter pyrex cylinder, ground on both ends, was clamped between rubber gaskets (lubricated with silicone grease) mounted in brass plates at the top and bottom of the chamber.

---

\* J. H. Johnston, S.M. Thesis, Metallurgy Department, M.I.T., 1951.

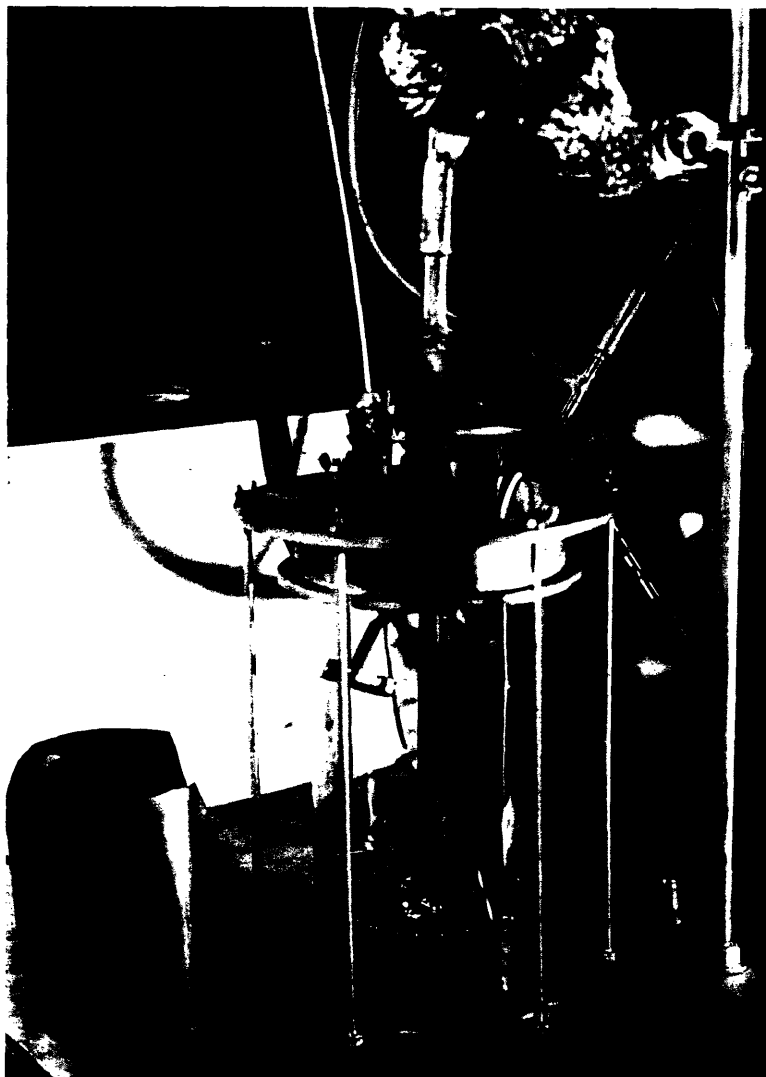


Fig. 10 - Arc melting chamber.



e. Wiper: A strip of silicone rubber was mounted on a steel rod and moved vertically along the inside surface of the cylinder to remove the sprayed metal dust which obscured vision during melting.

f. Seals: The electrode column and wiper rod moved vertically through lubricated rubber packing glands; the gland for the electrode was mounted on a silphon bellows to allow lateral electrode movement. Leakage through the glands while the chamber was under vacuum was very slight, but to eliminate this source of contamination, an evacuated seal around the wiper rod and an evacuated rubber sleeve around the electrode column and silphon bellows were added. The gripping action of the evacuated sleeve also prevented excessive strain on the bellows due to pressure increases in the chamber during melting.

g. Vacuum: A mechanical pump capable of attaining less than 1 mm. mercury pressure was used to evacuate the chamber and (separately) the sleeves. A mercury manometer was connected directly to the chamber.

h. Atmosphere: Helium, at 1 or 2 centimeters mercury positive pressure, was passed through a U-tube at -37 C, a vycore tube containing calcium turnings (resting on nickel sheet) at 650 C, and a trap containing activated charcoal at -187 C before entering the chamber.

## 2. Procedure:

Intended to eliminate all atmospheric contamination of the samples during melting, a typical sequence of operations follows:

a. Charging: The weighed amounts of titanium sponge and small pieces of 3/16 inch carbon electrode were placed in the bottom of the largest indentation in the plate, and the one or two blocks of nickel used in the charge were placed on top. The two small indentations in the plate were filled with titanium sponge.

b. Preparation: The chamber was assembled, the cylinder carefully fitted between the gaskets, and the chamber alone evacuated. The top plate was clamped tightly onto the cylinder. Helium was flushed through the purifying train and chamber. The charcoal trap was closed off from the rest of the purifying train, which was kept under a positive pressure, and the charcoal (and chamber) were evacuated while the charcoal was heated at 450 C for one hour. Then the charcoal was cooled slowly to -187 C, sealed from the chamber, and helium was allowed to enter the trap. A stopcock between the chamber and vacuum line was then closed, and the seals at the top of the chamber were evacuated. Helium was allowed to enter the chamber from the purifying train over a period of about twenty minutes, until a slight positive pressure was achieved in the chamber. Then the chamber was closed off from the trap, and the water to the electrode column and crucible was turned on.

c. Gettering: The closed atmosphere to be used for melting the sample was gettered by melting successively several small buttons from the sponge in the small indentations. The titanium was kept molten for one or two minutes.

d. Melting: The charge was melted down and kept molten until all of the graphite floating on the surface of the bath had disappeared. Then the ingot was turned over by manipulating the electrode, the sprayed dust on the inner wall of the chamber was partly removed by manipulating the wiper rod, and the ingot was remelted. One more remelting was usually sufficient to produce homogeneity in each ingot. Since nickel evaporation under the arc was severe, no more power was used than was necessary to keep the ingot completely liquid. The pressure increased during melting, but one atmosphere was not exceeded with an originally full chamber of gas except in the highest carbide samples. When melting was completed, the water was shut off for a few minutes prior to opening the chamber to minimize condensation on cold metal surfaces. The crucible surface was cleaned with acetone prior to the next charging operation.

The procedure described above was followed in subsequent operations with the exception of the activation of the charcoal, which was repeated every four or five melts. The chamber was always flushed with helium once or twice after opening it to the air.

D. Data on Important Compositions.

No.	% loss during melting	charge pct by weight.		ingot pct by weight		atomic pct calculated		melt No.
		<u>C</u>	<u>Ti</u>	<u>C</u>	<u>Ti</u>	<u>C</u>	<u>Ti</u>	
1*w	6.89	0.52	2.14	<u>0.39</u>	1.56	1.9	1.9	D25
2*w	3.46	1.99	8.15	<u>1.73</u>	6.98	7.8	7.9	C10
3*	----	2.69	11.00	<u>2.59</u>	10.42	11.3	11.4	13.7
4*w	10.67	3.59	14.70	<u>3.67</u>	14.83p	15.3	15.5	C18
5	7.10	2.14		2.30		10.5		NG2
6	9.60	6.35		6.75		26.4		NG1
7w	0.17		15.46		15.49		18.3	F16
8	0.47		16.25		16.32		19.4	F10
9	1.10	0.49	2.93	<u>0.51</u>	<u>2.91q</u>	2.4	3.5	F33
10	2.49	0.61	3.21	<u>0.88</u>	3.30	4.1	3.9	F1
11	0.07	0.70	3.26	<u>0.62</u>	<u>4.29</u>	2.9	5.1	F2
12	3.96	1.20	2.30	<u>1.29</u>	<u>2.50</u>	6.0	2.9	F26
13	0.67	1.00	4.00	<u>1.15</u>	4.03	5.3	4.7	F27
14	1.30	0.90	5.20	<u>0.91</u>	<u>5.31</u>	4.3	6.2	F28
15	0.51	0.80	6.69	<u>0.79</u>	<u>6.64</u>	3.7	7.8	F29
16	1.08	0.60	8.08	<u>0.72</u>	8.16	3.4	9.6	F30
17	0.44	0.35	10.00	<u>0.39</u>	<u>10.12</u>	1.8	12.0	F31
18	0.29	0.25	11.40	<u>0.25</u>	<u>11.41</u>	1.2	13.5	F32
19	2.00	3.54	8.12	<u>3.62</u>	8.29	15.3	8.8	F13
20	2.10	2.67	7.58	2.73	7.74	11.8	8.4	F6
21	0.58	2.20	8.98	<u>2.32</u>	9.05	10.2	10.0	F5
22	2.42	1.75	9.70	<u>1.91</u>	<u>9.70</u>	8.5	10.8	F4
23	0.77	2.00	10.51	<u>2.06</u>	<u>10.42</u>	9.2	11.6	F8
24	0.66	1.50	11.20	<u>1.46</u>	<u>11.23</u>	6.6	12.7	F3
25	1.19	1.20	12.26	<u>1.32</u>	12.41	6.1	14.3	F17
26	1.11	1.30	11.81	<u>1.26</u>	<u>11.92</u>	5.6	13.3	F18
27	0.73	1.06	12.61	<u>1.05</u>	12.70	4.8	14.6	F9
28	0.68	0.60	13.45	<u>0.59</u>	13.55	2.6	14.9	F19
29	0.35	0.80	14.32	<u>0.88</u>	<u>14.48</u>	4.0	16.6	F12
30	1.59	0.40	15.08	<u>0.60</u>	<u>15.40</u>	2.8	17.8	F14
31	4.95	5.01	20.54	<u>5.48</u>	<u>21.5</u>	21.2	20.9	F20
32	4.10	4.40	22.23	<u>4.66</u>	<u>23.1</u>	18.5	22.9	F21
33	5.05	3.75	22.46	<u>3.77</u>	<u>22.5</u>	15.7	23.0	F7
34	6.25	3.90	23.71	<u>3.51</u>	<u>25.9</u>	14.3	26.6	F22
35*		18.74	76.50	<u>21.2t</u>	78.0r	51.7	47.9	G3
				<u>1.9f</u>				

## Notes:

\*: prepared from a TiC - Ni powder mixture.

w: melted with a tungsten electrode.

—: value obtained by chemical analysis.

p: contained 81.0 pct nickel.

q: contained 95.0 pct nickel and 0.53 pct iron.

r: contained 0.80 pct nickel, 1.9 pct free carbon, and 21.2 pct total carbon.

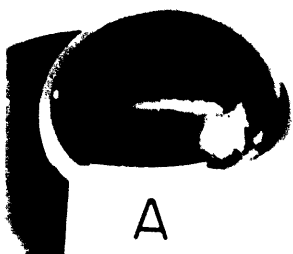
### E. Appearance of Ingots.

Figure 11 illustrates the appearance of some typical ingots after melting. Immediately after removal of the arc, a skin solidified over the surface of the sample; the features of this skin varied with the composition. In pure nickel, titanium, and the binary nickel-titanium melted with a tungsten electrode, the surface of the button was smooth and metallic. In most ternary compositions, however, particles visibly formed and floated to the surface of the liquid, uniting to form a dull crust at temperatures considerably above the heat evolution associated with the quasi-eutectic formation. In compositions close to the binary eutectic (G and H) the crust shrunk around the sample on cooling to form a continuous, wrinkled envelope; in hypoeutectic compositions (E) only a few particles formed to produce a "flower" on the top of the sample. In hypereutectic compositions (C, J-L), tiny particles nucleated large, shiny grains on the surface (Figure 12). With the exception of a slight segregation in carbide at the center of the ingot, the interior structure was uniform and bore no relation to the surface appearance. Shrinkage cavities within an ingot were never encountered.

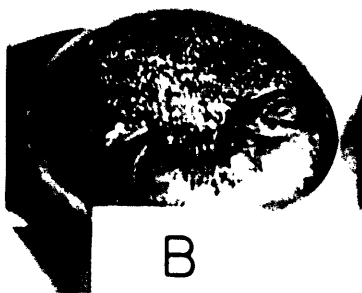
It is possible that some skin characteristics are due to nucleation of carbide particles by oxygen or nitrogen rich phases which would float to the surface at temperatures above the liquidus for TiC. Figure 13 shows that such phases do form at higher temperatures than TiC and then nucleate the carbide. The particle illustrated contains the "pink" phase associated with contamination at the center and is surrounded by light grey TiC. This structure was found in the

Fig 11: Typical ingot surfaces.

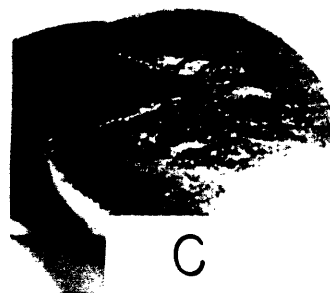
- A. Pure titanium.
- B. 18.3 atomic pct Ti, bal Ni (tungsten electrode).
- C. 15.3 atomic pct C, 8.8 atomic pct Ti, bal Ni.
- D. 6.0 atomic pct C, 2.9 atomic pct Ti, bal Ni. (contains no TiC)
- E. 4.3 atomic pct C, 6.2 atomic pct Ti, bal Ni.
- F. 1.8 atomic pct C, 12.0 atomic pct Ti, bal Ni (liquid TiC electrode).
- G. Approximately 4.8 atomic pct C, 14.6 atomic pct Ti, bal Ni.
- H. 6.6 atomic pct C, 12.7 atomic pct Ti, bal Ni.
- I. 10.2 atomic pct C, 10.0 atomic pct Ti, bal Ni.
- J. 21.2 atomic pct C, 20.9 atomic pct Ti, bal Ni.
- K. 14.3 atomic pct C, 26.6 atomic pct Ti, bal Ni. (Contains  $\text{TiNi}_3$ ).
- L. 11.5 atomic pct C, 29.0 atomic pct Ti, bal Ni (contains TiNi).



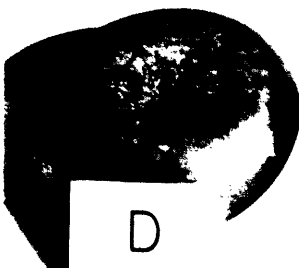
A



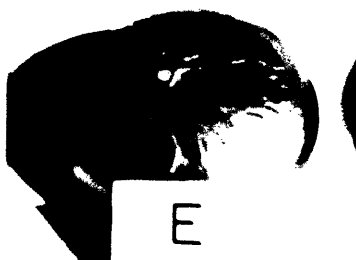
B



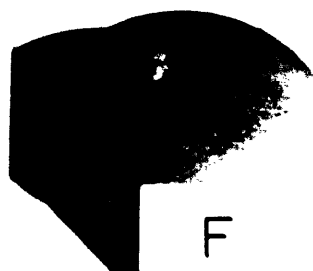
C



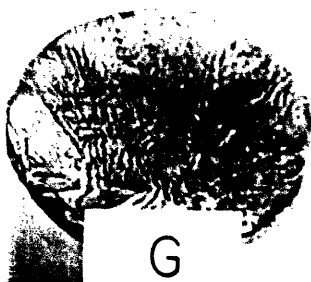
D



E



F



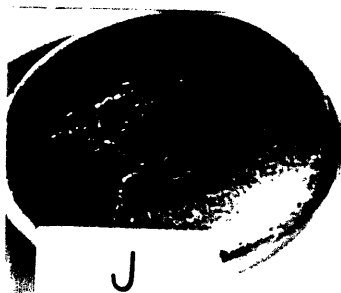
G



H



I



J



K



L



Fig 12 - Surface of Fig 11 J (21.2 atomic pct C, 20.9 atomic pct Ti, bal Ni) at 450 X. Structure unaffected by a nickel etching reagent. Note how particles of another phase have nucleated large TiC grains over the surface.





Fig. 13 - Particle in the nickel-titanium binary sample melted with a graphite electrode; the dark phase in the center is the "pink" structure associated with oxygen and nitrogen contamination, while the surrounding material is identical in appearance to light grey TiC. Alpha plus  $\text{TiNi}_3$  matrix. Particle unattacked by Carapella's reagent. 1500 X.

nickel-titanium binary alloy melted with the graphite electrode; the binary alloy melted with the tungsten electrode contained only yellow TiN or TiC particles.

## F. Chemical Analysis

While the carbon and titanium weights in the final ingots did not usually vary more than 1 or 2 per cent from the weights in the charge, the possibility of additions from the carbon electrode made analysis of this element essential in most cases. Analysis for titanium was also made in important compositions.

### 1. Sampling:

Chips for analysis were obtained by machining the sectioned surface of one half of each ingot, using a steel or carbide tool bit. Usually a few more chips were taken from the outer rim than from the center, to partially compensate for the slight increase in free carbide at the center of the ingot. Only in the case of the compositions containing large amounts of primary carbide was segregation of the phases in different regions of the ingot so severe as to cast doubt on the representative nature of the samples for analysis.

### 2. Carbon:

Carbon was obtained by combustion. A one-gram sample was fluxed with one gram of ingot iron, and the resulting material was ignited in a stream of oxygen for 10 to 12 minutes at 1350 C. The  $\text{CO}_2$  obtained was absorbed in askarite and weighed. The amount of carbon in the ingot iron was also determined and subtracted from the total.

### 3. Titanium:

The sample was dissolved in acid, the solution was diluted, and the titanium was precipitated with cupferron. The precipitate was filtered, washed, and ignited, and the  $\text{TiO}_2$  obtained was weighed. The result was corrected for nickel and iron carried along in the

precipitate by colorometric analysis for these elements. The amount of iron in the samples was usually about 0.05 per cent by weight.

### G. Preparation of Zirconia Boats

Stabilized zirconia boats were specially prepared for the heat treatment. This refractory ( $\text{ZrO}_2$  plus about 5 per cent  $\text{CaO}$  to inhibit solid phase transformations) has been used in melting titanium alloys, although it is not as inert as beryllia or thoria, which were unavailable.

The boats were pressed in a single-action die at about twelve tons per square inch from -350 mesh powder mixed with a 15-volume per cent solution of carbowax dissolved in benzene. Presintering was conducted by heating the compacts slowly, over a 3-hour period, to 1200 C and maintaining that temperature for one hour. The boats were then fired at 1800 C for several hours.

As fired in air, the refractory is a bright yellow color; but when it is heated in vacuum or a neutral or reducing atmosphere, the color tends towards a metallic black. Any of the refractory in contact with titanium or a liquid solution containing titanium also turns black to a depth of several millimeters. Upon reheating in air, the original color is restored. Consequently, in order to reduce the evolution of oxygen and nitrogen from the refractory during the heat treatment, the boats were given a pre-reducing treatment in hydrogen at 1000 C prior to use.

## H. Heat Treatment Equipment and Procedure

### 1. Equipment:

Figure 14 illustrates the conditions under which the samples were heat treated. Two 3/8-inch diameter "globars", having 5-inch hot zones, were heated by current from a 110 volt, 40 amp variac. The zircon (zirconium silicate) furnace tube, 30 inches long and 1-1/4 inches inside diameter, was sealed at both ends by rubber stoppers. A glazed porcelain thermocouple tube and a gas inlet tube entered the rear stopper; the front stopper contained a window and a glass tube connected to a short rubber hose, which was pinched around a molybdenum manipulating rod entering the furnace through the tube.

The atmosphere was helium purified through a U-tube at -37 C and calcium chips at 650 C. The gas also passed a flowmeter and mercury manometer before entering the chamber. The only detectable leaks in the system were through the front stopper assembly, and the gas was kept under a positive pressure of 1 or 2 inches of mercury whenever possible.

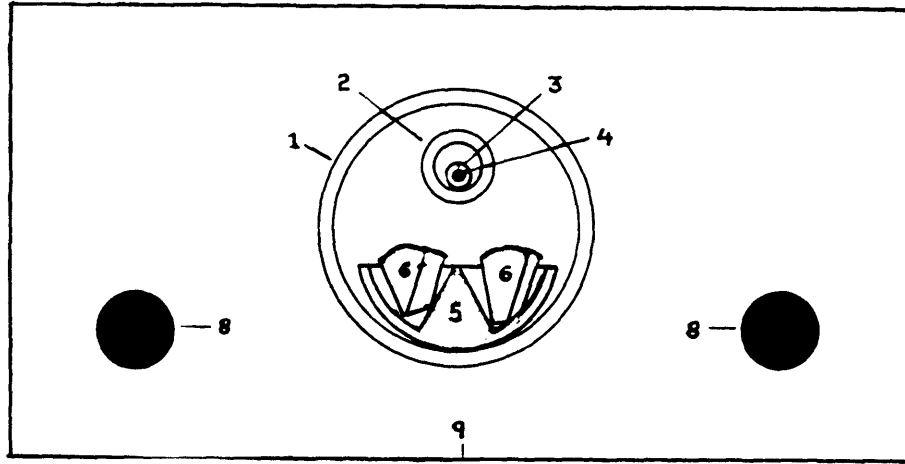
The temperature was measured by a platinum - 10 per cent rhodium thermocouple which had been annealed before use at 1000 C for about 30 minutes. The thermocouple was calibrated before the experiments by measuring the temperature at which gold wire, fused to the ends of the wires, melted. A measured temperature 1 degree below the melting point of gold was obtained. After most of the experiments had been made, another calibration was made by measuring a cooling curve on high purity copper (from the National Bureau of Standards) in graphite. The temperature measured at the beginning of the arrest was 2 degrees below the

Fig 14 - Arrangement of apparatus for heat treating samples (actual size):

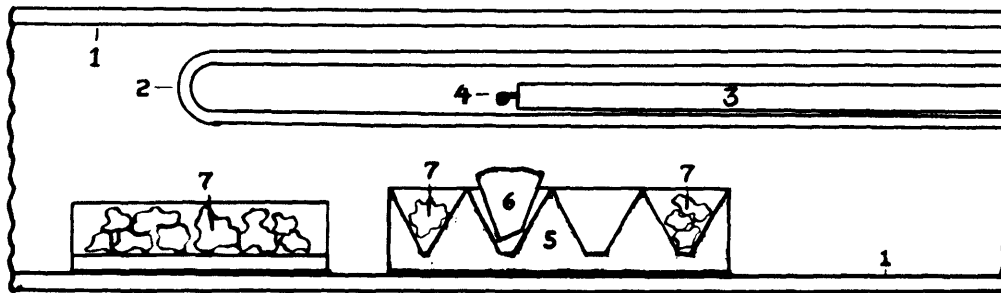
- (A) Transverse section;
- (B) Longitudinal section;
- (C) Typical temperature gradient.

Key:

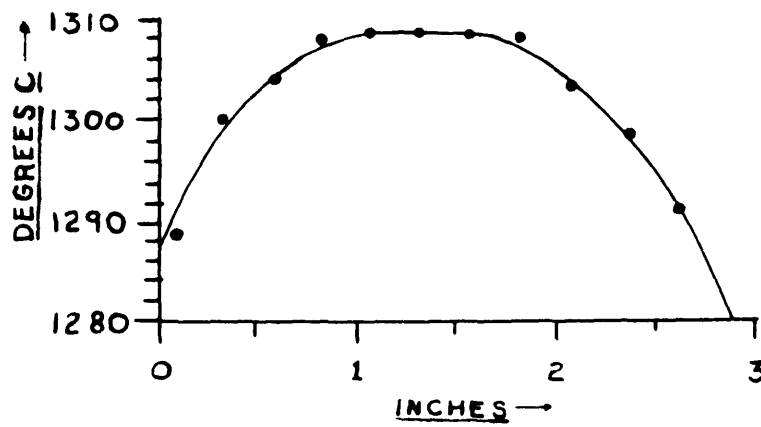
- (1) zircon furnace tube
- (2) porcelain protection tube
- (3) porcelain insulator
- (4) platinum - rhodium thermocouple
- (5) zirconia boat
- (6) sample wedges
- (7) titanium sponge
- (8) globars
- (9) furnace lining



A



B



C



melting point of copper. All of the temperatures measured in the experiments were finally raised 2 degrees C as a standard correction. An ice water cold junction was used throughout, and the millivoltages were recorded to within about 1 degree C by a Brown potentiometer.

## 2. Procedure:

Two or four wedges from the ingots were placed in the central indentations in the boats, and titanium sponge was placed in the other indentations as shown in Figure 14. Several boats were inserted into the rear half of the furnace tube, helium was allowed to flow through the chamber for about an hour, and then a controlled leak around the molybdenum rod in the front stopper was closed, allowing the pressure to build up to one or two inches of mercury. The furnace was brought slowly to the desired temperature, the gradient in the tube was measured, and the first boat was moved to a position at which the samples were in the constant temperature region of the furnace. Due to differential resistance changes in the globars with continued use, this constant temperature region shifted slightly between each series of experiments; however, it was possible in almost every case to move each set of samples to exactly the same position with respect to the gradient.

Manual control was found to be the most sensitive available method for maintaining constant temperature during the heat treatment of each boat load of samples. The temperature was recorded every 2 to 5 minutes, and the power input to the globars increased or decreased slightly, as necessary. By this method, it was possible to keep the temperature to within 2 or 3 degrees C of the desired temperature for at least 20 or 30 minutes before quenching.

Whenever a boat was to be quenched, the front stopper was removed, and the boat was quickly pulled into a pan of water with a molybdenum rod. (Samples containing liquid evolved heat down to a surface temperature of 700 - 800 C.) As soon as a boat was quenched, an alundum tray containing titanium sponge was inserted, and the front stopper was replaced. Gas was allowed to flow through the controlled leak for a few minutes before the tray of sponge was pushed into the heated region of the furnace tube and the next boat moved into position. Then the leak was closed, the pressure was allowed to build up again, and the temperature was brought to the next point of measurement.

The top of each sample (originating from the outside edge of the ingot) was somewhat cooler than the tip, due to radiation to the cold regions of the furnace; however, these temperature gradients within each piece usually were not great enough to produce different structures in different regions of the sample, and the wedges were always sectioned such that the central section of the wedge could be examined. Decarburization and oxidation were always confined to a narrow rim around the edge of the samples and did not affect the structure except when very large amounts of liquid were present.

Comparison of the measured temperature with the true temperature of the sample was made in several ways. In one case, beads of two chromel-alumel thermocouples were imbedded in holes in the sides of two typical samples heated to 1240 C. The positions of the beads should have represented the extremes in temperature encountered. By comparison with another thermocouple in the protection tube, it was found that the

temperature in one case was 4 degrees above the measured temperature, and, in the other case, 2 degrees below. Two pieces of 1/4 inch electrical copper plate ground to typical specimen shape were also placed side by side in the indentations. The sample on one side melted at 1079 C; while that on the other side melted at 1083 C. (One globar was at a higher temperature than the other in this test.) Blocks of the high-purity nickel ingot, treated in a similar manner, melted at temperatures 1 to 2 degrees above the melting point of nickel (1455 C) after 20 minutes at temperature. The measured temperatures (corrected for thermocouple calibration) were then taken as the correct temperatures, with a probable error of absolute temperature of 4 degrees C. The solidus temperatures of several compositions were reproduced to within this error.

For the runs at 1240 and 1190 C, samples were packed into a nickel boat 1 inch long and shaped to fit the inside of the chamber. Temperature in these runs was controlled to within 6 degrees C by an on-off Foxboro controller by-passing a 1 ohm resistor in series with the transformer.